doi:10.25143/prom-rsu_2021-04_dts

Rīga Stradiņš University

Arvīds Jakovļevs

Immunohistochemical Classification of Diffuse Gliomas

Summary of the Doctoral Thesis
for obtaining a doctoral degree (*Ph.D.*)

Sector – the Basic Sciences of Medicine, including Pharmacology

Sub-Sector – Pathology

Riga, 2021

Arvīds Jakovļevs

ORCID 0000-0002-9703-4922

Immunohistochemical Classification of Diffuse Gliomas

Summary of the Doctoral Thesis
for obtaining a doctoral degree (*Ph.D.*)

Sector – the Basic Sciences of Medicine,
including Pharmacology

Sub-Sector – Pathology

Riga, 2021

The Doctoral Thesis was developed at Rīga Stradiņš University, Latvia

Supervisor of the Doctoral Thesis:

Dr. habil. med., Professor **Jānis Gardovskis**,
Rīga Stradiņš University, Latvia
Dr. med., Professor **Ilze Štrumfa**,
Rīga Stradiņš University, Latvia

Official Reviewers:

Dr. habil. med. Professor **Māra Pilmane**,
Rīga Stradiņš University, Latvia
Dr. med., Associate Professor **Ave Minajeva**,
Tartu University, Estonia
Dr. med., Professor **Arvydas Laurinavicius**,
Vilnius University, Lithuania

The defence of the Doctoral Thesis will take place at the public session of the Promotion Council of the Basic Sciences of Medicine, including Pharmacology on 10 June 2021 at 12.00 held online via Zoom platform

The Doctoral Thesis is available in RSU Library and on RSU website: https://www.rsu.lv/en/dissertations

Secretary of the Promotion Council:

Dr. med., Professor **Juta Kroiča**

Table of contents

List of abbreviations

Ag	antigen
CD	cluster of differentiation
CI	confidence interval
CNS	central nervous systhem
DA	diffuse astrocytoma
GBM	glioblastoma
HE	haematoxilin and eosin stain
IDH	isocitrate dehydrogenase
IHĶ	immunohistochemistry
IQR	interquartile range
MVD	microvascular density
NA	not applicable
PDGFRA	platelet-derived growth factor receptor alpha
WHO	World Health Organization
SD	standard deviation
TCGA	The Cancer Genome Atlas
MRI	magnetic resonance imaging

Introduction

Glioblastoma (GBM) is one of the most common and aggressive tumours of the central nervous system (CNS) and represents the highest grade (grade IV) of glioma. Despite the standard therapy with maximal possible resection, followed by radiotherapy and chemotherapy with temozolomide, the prognosis of GBM patients remains dismal, with a median survival of 12–15 months (Stupp *et al.*, 2005). Total surgical resection of GBM is not possible because of the extensively infiltrative behaviour of neoplastic cells, and thus the recurrence of the tumour is inevitable (Roy *et al.*, 2015). The potential of chemotherapy and radiotherapy is also limited because of the resistance of tumour cells to standard therapy, and the fact that a haematoencephalic barrier is a major obstacle to chemotherapy. Because of the limited treatment options it is important to identify new molecular and immunohistochemical prognostic markers that can improve the treatment and even stratify patients into different prognostic groups, which will make the therapy more personalized for individual patients. Identification and research of potential molecular and immunohistochemical markers will help in better understanding critical molecular changes in tumorigenesis and increase the possibility of effective molecularly targeted therapy in future.

There are few reliable prognostic markers in GBM: for example, O6-methylguanine-DNA methyltransferase (MGMT) promoter status and *IDH1* gene mutations are currently almost the only available clinically relevant prognostic and predictive markers (Hegi *et al.*, 2005; Kaminska *et al.*, 2019; Kim and Liau, 2012). The most common *IDH1* gene mutation, IDH1 R132H, can also be easily detected by immunohistochemistry (IHC) for the IDH1 R132H mutant protein (Thota *et al.*, 2012).

The critical proteins (CD44, Ki-67, p53, p21, p27) involved in the hallmarks of the cancer such as invasion, proliferation and cell cycle regulation have been studied extensively, however the data is contradictory regarding the

prognostic role of these markers and more researches are necessary in this area (Le Mercier *et al.*, 2012; Popova *et al.*, 2014). There are a lot of discussions regarding the prognostic role of glioma stem cell markers such as CD133 and CD44 (Bhat *et al.*, 2013; Dong *et al.*, 2019; Hermansen *et al.*, 2011; Ortensi *et al.*, 2013). A lot of research is directed towards elucidating the molecular and genetic basis of GBM. Nowadays, new high-throughput molecular techniques have emerged that allow genome sequencing, expression profiling and epigenetic analysis to be carried out. To date, due to high-throughput genetic studies, emerging data have indicated the existence of several molecular subtypes in GBM. Verhaak *et al.* found that GBMs can be divided into four molecular subtypes, namely classical, mesenchymal, proneural and neural subtypes characterized by different molecular alterations and gene expression patterns (Verhaak *et al.*, 2010). Each subtype is characterized by certain genetic abnormalities, *IDH1* and *TP53* gene mutations and *PDGFRA* gene amplification in the proneural subtype, that correlated with better prognosis and younger age. However, more aggressive adjuvant treatment did not have an effect in this subtype, *EGFR* gene amplification is frequent in the classical subtype, *NF1* gene deletion and expression of genes specific to mesenchymal tissues (*CD44, MET, YLK-40*) characterized the mesenchymal subtype, but expression of neuron-specific genes (*NELF, GABRA*) typical of the neuronal subtype of GBM (Verhaak *et al.*, 2010). Other attempts at molecular subtyping of gliomas have been described and there is some overlapping of results and similarities among molecular subtypes identified across different studies (Brennan *et al.*, 2009; Liang *et al.*, 2005; Phillips *et al.*, 2006; Teo *et al.*, 2019). The unsolved issue is how to implement all these molecular data in routine clinical practice. GBM subtyping is possible and promising in routine practice but molecular data must be transformed into a more simplified and cheaper approach for daily practice and IHC might be a less expensive analogue of comprehensive and time-

consuming molecular analysis. There are few studies related to the utility of IHC in molecular subtyping of gliomas. For example, Le Mercier *et al*. distinguished proneural-like and classical-like GBM subtypes based on IHC for only three proteins: EGFR, PDGFRA and p53. They confirmed better survival in patients with proneural-like GBMs, whereas patients with classical-like GBMs benefited more from aggressive treatment (Le Mercier *et al.*, 2012). For evaluating the practical role of IHC in molecular subtyping of gliomas as well as for drawing conclusions on the prognostic or predictive role of separate potential IHC markers, more studies are essential.

The **aim** of this research was to evaluate the morphological and immunohistochemical profile of gliomas – glioblastoma (GBM) and diffuse astrocytoma (DA) – as well as to evaluate the prognostic role of single immunohistochemical markers and the possibility of glioma subtyping by IHC in gliomas.

In order to achieve this aim, the following tasks were conducted:

1. Characterizing the morphological structure of gliomas.
2. Assessing angiogenesis by microvascular density (MVD) in GBMs and Das.
3. Assessing the proliferation fraction by Ki-67, as well as the expression of cell cycle regulators (p21, p27), aberrant p53 protein, PDGFRA and CD44 in GBMs and Das.
4. Assessing the frequency of IDH1 R132H mutation by IHC in GBMs and Das.
5. Evaluating correlations and associations between clinical, morphological and immunohistochemical parameters in GBMs and Das.
6. Assessing survival and factors that have an impact on it in GBMs and Das.

7. Assessing the possibility of immunohistochemical subtyping of gliomas and analysing interrelations with any clinical, morphological and immunohistochemical parameters.

Scientific hypothesis

- Morphological and immunohistochemical characteristics have a prognostic role in GBMs.
- Subtyping of GBM is possible through the application of immunohistochemistry.
- **Scientific novelty:**
- In this study, several immunohistochemical markers will be evaluated concerning what contradictory and insufficient scientific evidence exists in the literature.
- In this study, the hypothesis as to whether IHC-based classification is possible for gliomas will be tested.
- This work is the first study in Latvia in which a comprehensive evaluation of GBM morphological and immunohistochemical characteristics and survival has been performed.

Personal contribution

The author has conducted all stages of the study, including preparation of the study design and selection of IHC markers, as well as evaluating the IHC results, scientific measurements and statistical data analysis. The author also performed the immunohistochemical visualization and took all the gross and microscopical photographs presented in this work.

Ethical concerns

This research was carried out in accordance with the Declaration of Helsinki and received approval from the Committee of Ethics of Rīga Stradiņš University, No E-9 (2), 12.09.2013.

1. Materials and methods

1.1. The essence of study

This thesis was performed as a retrospective study based on the analysis of formalin-fixed, paraffin-embedded, surgically treated human glioma tissues. The cases were identified through an archive search of all consecutive patients (2009–2014) who were subjected to neurosurgical treatment by routine indications in a single university hospital (Pauls Stradins Clinical University Hospital, Riga). Comprehensive morphological and immunohistochemical evaluations of 172 gliomas were performed, including 146 GBMs (WHO grade IV) and 26 DAs (WHO grade II). Anaplastic astrocytomas (WHO grade III) were excluded from the study because we evaluated the two most contrasting grades of diffuse gliomas. The research was carried out in accordance with the Declaration of Helsinki and received approval from the Committee of Ethics of Rīga Stradiņš University, No E-9 (2), 12.09.2013.

1.2. Patient cohort and sample collection

The study included 172 gliomas; 146 consecutive cases of GBMs and 26 cases of DAs were identified by archive search from 2009 to 2014. Each tumour was classified according to the 2016 WHO classification of tumours of the CNS. Only those patients with diagnoses of DAs and GBMs that met the following inclusion criteria were included in the study.

1. Patients with histologically proved GBMs and DAs that were diagnosed according to the criteria defined by the 2016 WHO classification of tumours of the CNS.
2. A sufficient amount of tissue material (only surgical resection material).

3. Adequate tumour tissue material (comprised of at least 10% of tissue material composed from morphologically intact, non-necrotic tumour cells).
4. Newly diagnosed glioma cases without any preceding adjuvant therapy.

The exclusion criteria for the study were as follows:

1. Other histological types of glial tumours and tumours with doubtful histological appearance.
2. Small amount of tissue material or material acquired from brain stereotactic biopsies.
3. Seriously damaged and non-adequate tissue material: necrosis and/or tissue damage artefacts constitute more than 90% of tissue material.

Patients' demographic information (gender, age), data concerning tumour size and localization as well as the data about the adjuvant treatment (chemotherapy with temozolomide and/or radiotherapy) were acquired from medical case histories. Data about tumour size and localization was also verified from MRI descriptive reports.

1.3. Tissue processing and microscopy

Gross description are not essential when grossing brain tumours because the WHO classification system and grading of CNS tumours relies mainly on microscopical, immunohistochemical and molecular features but not gross examination. Thus, during grossing, only the amount of received tissue material were recorded and all available fragments of tissue material obtained from patients who were subjected to neurosurgical treatment were submitted for subsequent processing and microscopical analysis.

The tumour tissue samples were fixed in neutral buffered 10% formalin (Sigma-Aldrich, United States of America), processed in a Tissue-Tek® VIPTM

6 vacuum infiltration processor (Sakura Seiki Co., Ltd, Nagano, Japan) and embedded in paraplast (Diapath S.r.l., Belgamo, Italy) using a TES 99 tissue-embedding system (Medite GmbH, Burgdorf, Germany). After embedding, tissue samples from paraffin blocks were cut into 4-micron-thick sections with a microtome (Accu-cut SRM 200CW, Sakura Finetek Europa B.V., the Netherlands), put on glass slides (Menzel-Glaser, Braunschweig, Germany) and stained with haematoxylin and eosin (H&E) using an automated tissue stainer (TST 44, Medite Medizintechnik, Germany). The stained slides were covered by cover glass (Prestige, Vemi S.R.L., Milano, Italy) employing an automated coverslipper (Dako Coverslipper, Dako Denmark A/S, Glostrup, Denmark). Standard slides, stained with haematoxylin and eosin, were examined under a light microscope to obtain morphological data about the tumour histological type according to criteria defined by the 2016 WHO classification of tumours of the CNS, as well as to evaluate the quality and quantity of the tumour tissue material.

1.4. Immunohistochemistry

Immunohistochemical visualization was performed on formalin-fixed paraffin-embedded tissues of CNS glial tumours. First, each case stained by haematoxylin and eosin was evaluated under a light microscope to select the most qualitative and representative tissue block-based assessment of viable, non-necrotic tumour tissue assessible for immunostaining and subsequent microscopical analysis. Complete necrosis or disappearance of tumour tissue in the deeper sections prompted exclusion from immunohistochemical evaluation.

For IHC analysis, 3-micrometre-thick sections were cut using a Microm HM 360 electronic rotary microtome on electrostatically charged glass slides (Histobond, Marienfeld, Germany) followed by deparaffinization in graded alcohols (Sigma-Aldrich). Heat-induced antigen epitope retrieval was performed according to the manufacturer's instructions in TEG buffer at pH 9.0 using a

microwave oven for 3×5 min. After blocking endogenous peroxidase (Sigma-Aldrich), the sections were incubated with primary antibodies at room temperature. Each antibody used in immunohistochemistry was initially standardized using control tissue as recommended on their specification sheets. Positive controls were performed in accordance with data given by the company; negative controls were performed when the primary antibody was not applied. When an optimal concentration of antibody was found, it was tested on glioma tissues. The clonality, species origin and specificity as well as the working dilution and manufacturer are shown in Table 1.1.

Table 1.1.

Characteristics of primary antibodies

Antigen	Antibody characteristics	Clone	Dilution	Manufacturer
Ki-67	Monoclonal mouse Ab against human Ag	MIB-1	1:100	Dako
p53	Monoclonal mouse Ab against human Ag	DO-7	1:400	Dako
$p21^{WAF1/Cip1}$ protein	Monoclonal mouse Ab against human Ag	SX118	1:25	Dako
$p27^{Kip1}$ protein	Monoclonal mouse Ab against human Ag	SX53G8	1:50	Dako
Mutant IDH R132H	Monoclonal mouse Ab against human Ag	H09	1:50	Dianova
PDGFRA	Rabbit polyclonal Ab against human Ag	Polyclonal	1:200	Abcam
CD44	Monoclonal mouse Ab against human Ag	DF1485	1:50	Dako
CD34	Monoclonal mouse Ab against human Ag	QBEnd10	1:50	Dako

Abbreviations in the Table: Ab, antibody; Ag, antigen

After immunostaining, the expression of markers was evaluated by light microscopy under high-power magnification (400x).

The expression of markers was considered positive only if the expression intensity was moderate or high (Ryu *et al.*, 2018; van Diest *et al.*, 1997). The intensity levels are shown in Figure 1.1. on example of CD44 expression.

For most markers (Ki-67, p53, p21, p27, CD44, CD34) the presence of nuclear, cytoplasmic or membranous staining was assessed quantitatively as the relative number of positive neoplastic cells (%).

For PDGFRA, we used both a quantitative and a semi-quantitative method (0–9 % of immunoreactive cells were considered as the negative sample, with 10–50 % focally positive and > 50% positive). The expression of IDH1 R132H mutant protein was assessed only as positive (+) and negative (−) (Figure 1.2.).

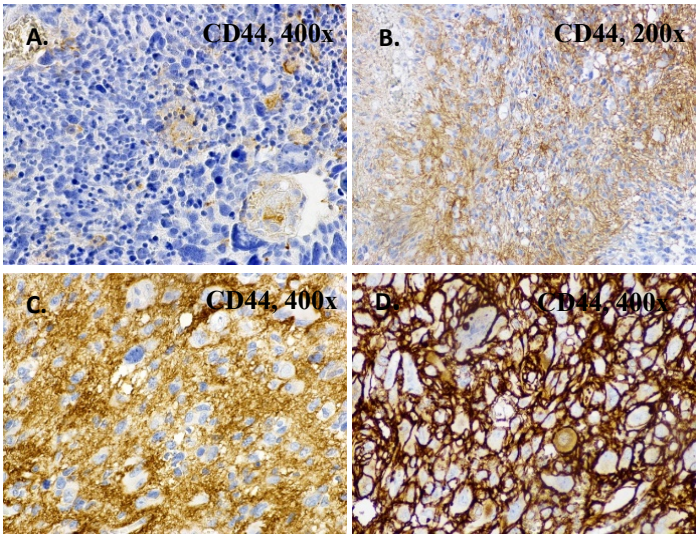

Figure 1.1. **The intensity levels of CD44 expression in GBM**
A, no expression; B, low expression; C, moderate intensity; D, high intensity. Immunoperoxidase, CD44, original magnification 200× (B) and 400× (A, C, D).

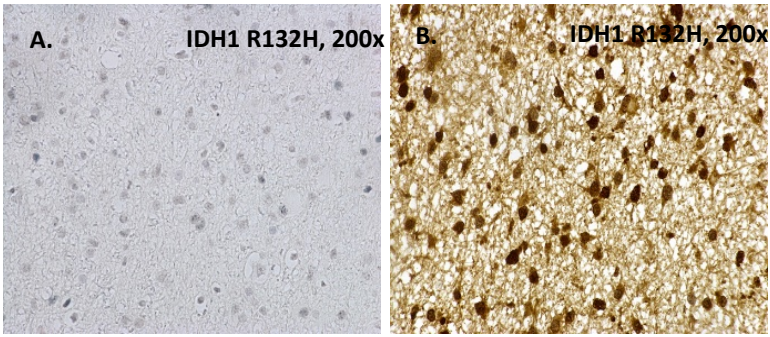

Figure 1.2. **Immunohistochemical visualization of IDH1 R132H mutant protein in Das**
A, negative; B, positive; Immunoperoxidase, IDH1 R132H, original magnification 200×.

To detect the MVD, endothelial differentiation was highlighted by CD34 expression. MVD was assessed according to Weidner's approach (Weidner *et al.*, 1991). The first step was the identification of a "hot spot" of increased microvascular density by light microscopy at low-power magnification (Figure 1.3.). Then individual microvessels were counted at high power in an adequate area (0.74 mm^2 per field at 400x) (Figure 1.4.). Each count was expressed as the highest number of microvessels found within 400x magnification. Vessels with muscular walls were not counted.

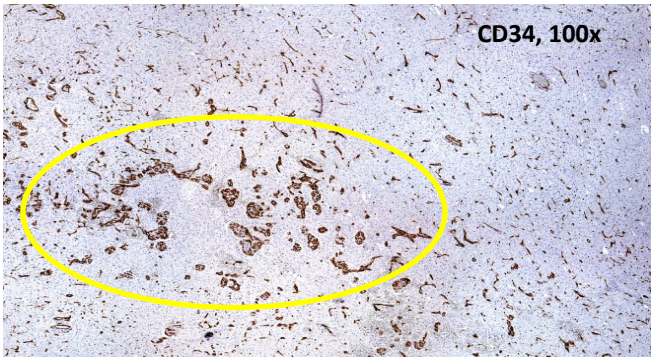

Figure 1.3. **Evaluation of MVD in GBM**
Hot spot area in yellow circle. Immunoperoxidase, CD34, original magnification 100×.

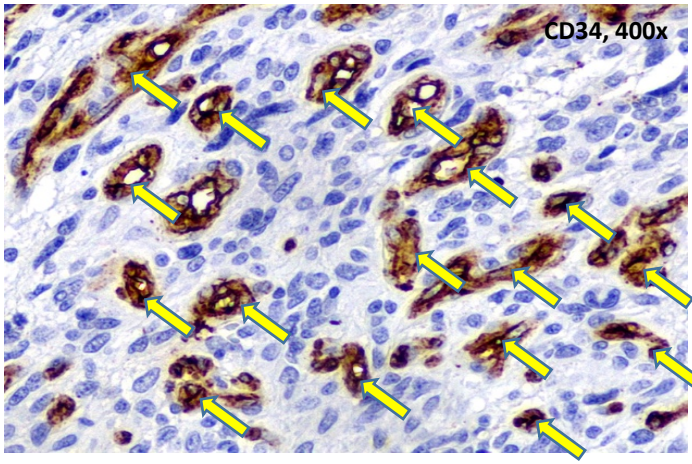

Figure 1.4. **Microvessels (arrows) in GBM**
Immunoperoxidase, CD34, original magnification 400×.

For each case to be considered positive, the relative number of positive cells had to reach a certain cut-off value. In the literature there were many disagreements regarding the best cut-off values in gliomas, and many authors used very different cut-offs. Thus, we used two cut-offs for each marker. The first cut-off value was based on other studies published in international journals, and secondly we used our own cut-off value based on the median expression value of immunohistochemical marker. For MVD, the cut-off was selected only based on the median value of expression because of the few studies in literature regarding the cut-off for CD34. The chosen cut-off values for immunohistochemical markers for both GBMs and DAs are shown in Table 1.2.

Table 1.2.

The cut-off values of immunohistochemical markers for GBMs and DAs

Marker	GBM	DA	References
Ki-67	25% and 41% (median)	3% and 5.5% (median)	(Jin *et al.*, 2011; Neder *et al.*, 2004)
p53	10% and 15% (median)	10% and 52% (median)	(Popova *et al.*, 2014; Wang *et al.*, 2014)
CD44	50% and 86.5% (median)	50% and 8.5% (median)	(Popova *et al.*, 2014)
PDGFRA	50% and 1% (median)	50% and 42% (median)	(Popova *et al.*, 2014)
p21	20% and 19% (median)	20% and 2.5% (median)	(Trabelsi *et al.*, 2016)
p27	70% and 74% (median)	70% and 92% (median)	(Faria *et al.*, 2007; Yang *et al.*, 2011)
MVD	35% (median)	13.0% (median)	NA

* Abbreviations in the table: NA, not applicable; MVD, microvascular density; PDGFRA, platelet-derived growth factor receptor alpha; GBM, glioblastoma; DA, diffuse astrocytoma

The immunohistochemical data of p53, IDH1 R132H, PDGFRA and CD44 expression was used to determine the subtype of GBMs (previously described by Verhaak *et al.*, *2010*). Based on these protein expression signatures three categories of GBMs were distinguished: proneural, mesenchymal and not otherwise classified, referred to as “Other”. The proneural subtype was defined by high expression of p53 and/or high expression of PDGFRA and/or positivity of IDH1 R132H. The mesenchymal subtype was defined by high expression of CD44 and low expression of proneural markers (p53, PDGFRA, IDH1 R132H). All remaining cases that do not fit the proneural or mesenchymal subtype category were called “Other” or not otherwise classified (see Figure 1.5).

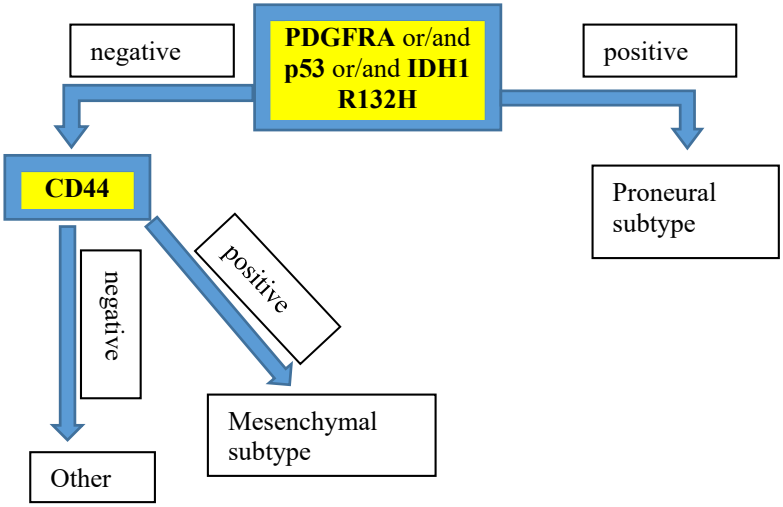

Figure 1.5. **Immunohistochemical subtyping of gliomas**

Analysis of immunostained specimens was carried out with a Carl Zeiss Axiolab (Germany) microscope. Nuclear immunostaining of Ki-67, p53, p21 and p27 was evaluated by computed morphometry using the Kappa image base program (KAPPA opto-electronics INC., United States of America).

1.5. Statistical analysis

All statistical analysis were performed with the IBM SPSS Statistics Version 20.0 statistical software package (International Business Machines Corp., Armonk, New York, USA). The assumption check of normality using the Shapiro-Wilk test was performed before statistical calculations. Descriptive statistics were calculated as mean ± standard deviation (SD), median with interquartile range (IQR) and/or frequency (%) with 95% confidence interval (CI). Descriptive statistical methods, including descriptive and cross-tabulation

with Pearson's chi-square, Fisher's exact test, bivariate correlation as Spearman's rank correlation coefficient, the non-parametric method including the Mann-Whitney U test and the Kruskal-Wallis one way analysis of variance by ranks, were used.

Survival was evaluated by Kaplan-Meier analysis. A p value of < 0.05 was considered statistically significant.

2. Results

2.1. Basic characteristics of research group

2.1.1. Characteristics of GBM cases

The study included 146 patients diagnosed with GBM during the evaluated period of time (2009–2014). GBM was diagnosed in 75/146 (51.4%; 95% CI = 43.3–59.5) females and in 71/146 (48.6%; 95% CI = 40.5–56.7) males. The age of patients ranged from 34 to 89. The mean age ± standard deviation (SD) was 62.0 ± 11.2 (95% CI = 60.2–63.8). The median age was 62.0 (IQR = 18). The mean age of males ± SD was 60.8 ± 11.5 (95% CI = 58.1–63.5); the median age was 60.7 (IQR = 19). The mean age of females ± SD was 63.1 ± 10.9 (95% CI = 60.7–65.7); the median age was 65.0 (IQR = 17).

The most frequent localization of GBM was the frontal lobe – 56/146 (38.4%; 95% CI = 30.5–46.3), followed by the temporal lobe – 41/146 (28.1%; 95% CI = 20.8–35.4), the parietal lobe 21/146 (14.1%; 95% CI = 8.5–19.7) and the occipital lobe 2/146 (1.4%; 95% CI = 0–3.3); 26/146 (17.8%; 95% CI = 11.6–24.0) GBM cases diffusively infiltrate several lobes in the same hemisphere; 78/146 (53.4%; 95% CI = 45.3–61.5) GBMs were localized in the right cerebral hemisphere, while 62/146 (42.5%; 95% CI = 34.5–50.5) GBMs were found in the left hemisphere; 6/146 (4.1%; 95% CI = 0.9–7.3) GBMs were bilateral involving both frontal lobes. Multifocal involvement was recognized in 16/146 (11.0%; 95% CI = 5.9–16.1) GBMs.

The maximum tumour diameter measured from the MRI series ranged from 1 to 9 cm; the mean ± SD was 5.1 ± 1.4 (95% CI = 4.85–5.36); the median was 5.1 (IQR = 2). In 101/123 (29.5%; 95% CI = 21.4–37.6) GBM cases the maximum diameter exceeded 4 cm. In 22/123 (15.1%; 95% CI = 8.8–21.4) GBMs the maximum diameter was less than 4 cm. The MRI data were missing for 23/146 (15.7%; 95% CI = 9.8–21.6) cases from the sample.

Surgical resection was performed in all GBMs (146/146), and in addition, adjuvant therapy such as radiotherapy or chemotherapy with temozolomide was used. The data about type of therapy was not available in 11/146 (7.5%; 95% CI = 4.3–12.9) cases. In the remaining 135 patients with GBM the most frequent therapy was the standard type of treatment with surgery followed by adjuvant radiotherapy and chemotherapy with temozolomide – 56/135 (41.5%; 95% CI = 33.5–49.9) patients; surgery plus radiotherapy was used in 50/135 (37.0%; 95% CI = 29.3–45.4) patients and 29/135 (21.4%; 95% CI = 15.3–29.1) patients did not receive any adjuvant oncological treatment and only surgical resection was performed. Patients receiving adjuvant temozolomide and radiotherapy were younger than those who received adjuvant radiotherapy or were treated with surgical resection alone without adjuvant treatment (one-way ANOVA, $p < 0.001$). The mean ages of patients receiving different types of treatment were 55.0 (95% CI = 52.5–57.5) years, 65.9 (95% CI = 62.9–68.7) years and 69.0 (95% CI = 65.3–72.7) years. There was no association between tumour size and type of treatment (Kruskal-Wallis H; $p = 0.708$).

2.1.2. Characteristics of DA cases

This study included 26 patients diagnosed with DA during the evaluated period of time (2009–2014). DAs were diagnosed in 14/26 (53.8%; 95% CI = 34.6–72.7) females and 12/26 (46.2%; 95% CI = 27.0–65.4) males. The age of patients ranged from 21 to 67. The mean age ± SD was 37.5 ± 11.2 (95% CI = 33.0–42.0). The median age was 35.5 (IQR = 19). The mean age of males ± SD was 37.6 ± 12.3 (95% CI = 29.8–45.5); the median age was 34.0 (IQR = 17). The mean age of females ± SD was 37.4 ± 10.5 (95% CI = 31.3–43.4); the median age was 36.0 (IQR = 20).

The most frequent localization of DA was the frontal lobe 13/26 (50%; 95% CI = 30.8–69.2), followed by the temporal lobe 6/26 (23.1%; 95% CI = 6.9–

39.3); 7/26 (26.9%; 95% CI = 9.9–43.9) DAs involved several cerebral lobes; 14/26 (53.8%; 95% CI = 34.6–72.0) DAs were localized in the right cerebral hemisphere, while 12/26 (46.2%; 95% CI = 27.0–65.4) DAs were found in the left hemisphere.

The maximum tumour diameter measured from the MRI series ranged from 4.7 to 9 cm; the mean ± SD was 6.1 ± 0.9 (95% CI = 5.6–6.7); the median was 6.0 (IQR = 1). The MRI data and information about tumour size were missing for 13/26 (50.0%; 95% CI = 30.8–69.2) cases from the sample.

Surgical resection was performed in all DAs (26/26); in addition, all patients received adjuvant radiotherapy.

2.2. Morphology

2.2.1. Characteristics of GBM cases

All GBM cases were diagnosed according to the 2016 WHO classification of CNS tumours and thus all cases showed necrosis (ischaemic and/or pseudopalisading) and microvascular proliferation (Figure 2.1), and IDH1 status was assessed by IHC.

In 16/146 (10.9%; 95% CI = 5.8–16.0) GBM cases, a mild, initial microvascular proliferation was found, however the presence of necrosis and cellular atypia supported a diagnosis of GBMs. In 130/146 (89.0%; 95% CI = 83.9–94.1) GBM cases microvascular proliferation was prominent, frequently with the formation of glomeruloid-like vascular structures.

Most GBM cases – 141/146 (96.6%; 95% CI = 93.7–99.5) – belong to conventional GBMs. There were only 2/146 (1.4%; 95% CI = 0–3.3) gliosarcomas and 3/146 (2.1%; 95% CI = 0–4.4) giant-cell GBMs.

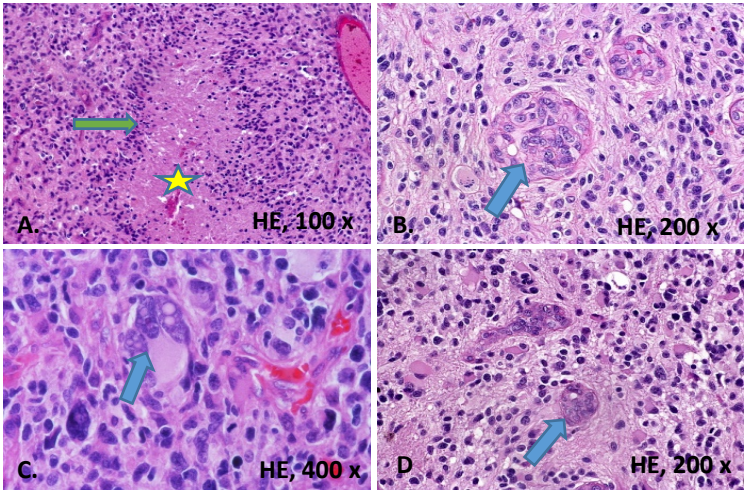

Figure 2.1. **Morphology of GBM**
A, pseudopalisading necrosis. Pseudopalisade is shown by green arrow; necrosis in the centre is shown by yellow star. B, glomeruloid microvascular proliferation (arrow). C, prominent cellular atypia and giant atypical cell (arrow). D, initial microvascular proliferation forming multilayer tufts of endothelial cells. Haematoxylin and eosin (HE), original magnification 100x (A), 200× (B, D) and 400× (C).

2.2.2. Characteristics of DA cases

All 26/26 (100%) DAs were diagnosed as diffuse fibrillary astrocytomas on morphological grounds according to the 2016 WHO classification of CNS tumours (Figure 3.9). All DAs showed mild to moderate cellularity; however, 3/26 (11.5%; 95% CI = 0 – 23.7) DAs showed focal areas of increased cellular density compared with the rest of the tumour, and rare mitotic figures up to 2 mitoses per 10 high-power field were found. All DAs showed mild nuclear atypia, no necrosis and no microvascular proliferation. In 2/26 (7.7%; 95% CI = 0–17.8) DAs prominent gemistocytic astrocytes were found; 12/26 (46.1%; 95% CI = 26.0–65.3) DAs showed microcystic changes. Morphological features of DAs are shown in Figure 2.2 (A–D).

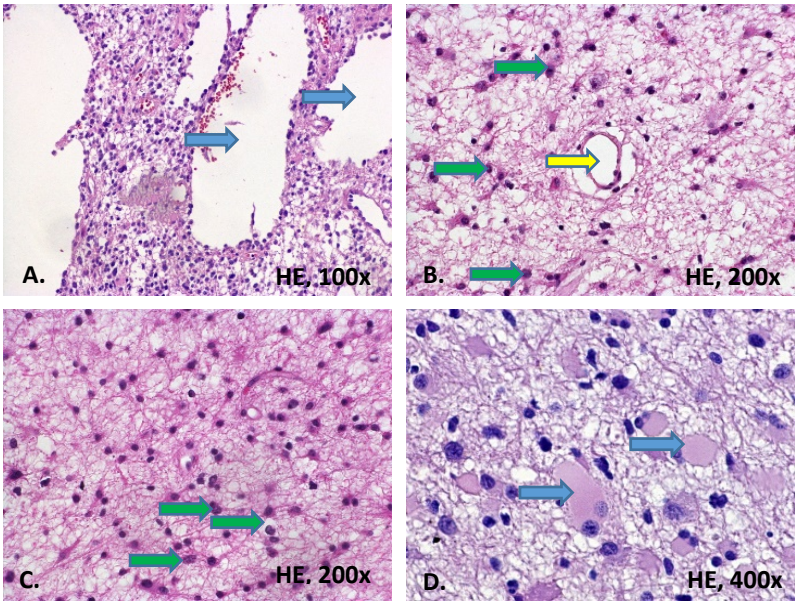

Figure 2.2. **Morphology of DA**
A, microcystic changes (blue arrows) B, C, mild cellularity; note small, uniform nuclei of neoplastic cells (green arrows) and microvessel (yellow arrow). D, Gemistocytic astrocytes; note enlarged, plump cells with abundant eosinophilic cytoplasm (blue arrows). Haematoxylin and eosin (HE), original magnification 100× (A), 200×(B, C) and 400× (D).

2.3. Immunohistochemical findings in GBMs and DAs

The expression of the following immunohistochemical markers was assessed in GBMs and DAs: Ki-67, p53, p21, p27, CD44, PDGFRA, IDH1 R132H and CD34.

Immunohistochemical results of all evaluated markers are summarized in Table 2.1. The expression of examined markers is shown in Figure 2.3.

The expression of p53 and Ki-67 was confined to the nuclei of neoplastic cells. GBMs demonstrated a marked increase in Ki-67 proliferation activity compared with DAs: 44.4% [95% CI = 41.1–47.6] versus 6.4% [95% CI = 4.7–8.0].

Ki-67 proliferation indices ranged from 13 to 95 % in GBMs and from 2 to 15 % in DAs.

The expression of the aberrant p53 protein varied significantly in both groups from absence of any immunoreactivity (0%) to strong labelling of almost all cells (99%). Some level of p53 immunoreactivity (> 1%) was found in 87.3% (95% CI = 81.5–93.1) of GBMs and 87.5% (95% CI = 74.3–100) of DAs. However, strong p53 immunoreactivity (> 50%) was found in 31.7% (95% CI = 23.6–39.8) of GBMs and 50% (95% CI = 30.8–69.2) of DAs. There was no statistically significant difference in p53 protein expression in analysis of the mean amount of positive cells between DAs and GBMs ($p = 0.416$). With the selected cut-off of 10%, p53 expression was found in 64.3% (95% CI = 55.6–72.1) of GBMs and 75.0% (95% CI = 55.1–88) of DAs.

Expression of p21 was significantly more frequent in GBMs than in DAs: 21.2% (95% CI = 18.7–23.6) versus 6.9% (95% CI = 2.4–11.4). Also, using a cut-off of 20%, 49.3% (95% CI = 41.3–57.4) of GBMs and only 15% (95% CI = 5.2–36.0) of DAs had a high expression of p21.

Expression of p27 was common in both GBMs and DAs, however the mean value of p27 expression was lower in GBMs than in DAs: 69.7% (95% CI = 65.8–73.7) versus 86.6% (95% CI = 81.6–91.7). Using the cut of 70%, a high p27 protein expression was found in 60.1% (95% CI = 50.9–68.7) of GBMs and 86.9% (95% CI = 67.8–95.4) of DAs.

CD44 protein was expressed in a significantly greater percentage of cells in GBMs than in DAs: 74.1% (95% CI = 69.6–78.7) versus 13.5% (95% CI = 7.7–19.2). All cases of GBMs and DAs showed some level of CD44 expression. A strong expression of CD44 in more than 50% of neoplastic cells was found in 81.5% [95% CI = 74.6–87.4] of GBMs compared with only one DA that reached this level of expression. Intense, diffuse membranous expression was the predominant pattern of CD44 immunoreactivity in GBMs. However, the

expression of CD44 in DAs was weak and mostly limited to numerous cytoplasmic processes of astrocytes creating a richly branched, delicate network of low CD44 immunoreactivity. In addition to this weak CD44 expression, all DAs had patchy areas with at least a moderate expression level of CD44.

Significantly, increased expression of PDGFRA was observed in DAs compared with GBMs ($p < 0.001$). A high PDGFRA protein expression was observed (with a cut-off of 50%) in 6.2% (95% CI = 5.0–10.6) of GBMs and 52.6% (95% of CI = 30.1–75.0) of DAs. PDGFRA in most cases was expressed in the cytoplasm and membrane of neoplastic cells; however, some rare cases showed nuclear labelling.

IDH1 R132H protein expression was found in 3.4% (95% CI = 0.5–6.3) of GBMs compared with 76.9% (95% CI = 60.7–93.1) of DAs. All cases showed intense nuclear staining. Among the positive GBM cases, only one GBM morphologically showed component of lower-grade glioma, thus confirming secondary GBMs on morphological grounds. All IDH1 R132H positive GBMs ($n = 5$) lacked any radiological or clinical evidence of a pre-existing low-grade tumour.

The microvascular density (MVD) was assessed by CD34 immuno-staining to highlight the endothelial cells. In GBMs, the MVD ranged from 6 to 130 microvessels per high-power field. The mean MVD ± SD was 40.7 ± 25.4 (95% CI = 35.8–45.6) and the median value was 35.0 (IQR = 29). In Das, MVD ranged from 4 to 49 microvessels per high-power field. The mean MVD ± SD was 18.1 ± 12.1 (95% CI = 12.9–23.3) and the median value was 13.0 (IQR = 16). Thus, MVD in GBMs was significantly higher than in DAs ($p < 0.001$).

Table 2.1.

IHC profile of GBMs and DAs

Variable	GBM	DA
Ki-67		
Number of evaluated cases	126	24
Mean ± SD; 95% CI	44.4% ± 18.5; 41.1–47.6	6.4% ± 3.9; 4.7–8.0
Ki-67		
Median; IQR	41.0; 24	5.5; 6
High Ki-67 expression; No; %; 95% CI (cut-off 25%)	111; 88.1 81.2–92.6	0; 0 0–10.3
High Ki-67 expression; No; %; 95% CI (cut-off 41%)	61; 48.4 39.8–57.0	0; 0 0.0–13.8
High Ki-67 expression; Number of cases; %; 95% CI (cut-off 3%)	126; 100% 97.0–100	16; 66.7 46.7–82.0
High Ki-67 expression; No; %; 95% CI (cut-off 5%)	126; 100% 97.0–100	12; 50.0 31.4–68.5
p53		
Number of evaluated cases	126	24
Mean ± SD; 95% CI	35.3 ± 37.6 28.7–42.0	43.4 ± 31.7 30.0–56.8
Median; IQR	15.0; 71	52.0; 63
0–5 % of p53 positive cells; No; %; 95% CI	30; 23.8 17.2–31.9	6; 25.0 12.0–44.9
6–10 % of p53 positive cells; No; %; 95% CI	25;19.8 13.8–27.6	0; 0 0–13.8
11–50 % of p53 positive cells; No; %; 95% CI	31; 24.6 17.9–33.2	6; 25.0 12.0–44.9
> 50% of p53 positive cells; No; %; 95% CI	40; 31.7 24.2–40.3	12; 50.0 31.4–68.6
High p53 expression; No; %; 95% CI (cut-off 10%)	81; 64.3 55.6–72.1	18; 75 55.1–88
High p53 expression; No; %; 95% CI (cut-off 15%)	67; 53.2 44.5–53.2	17; 70.8 50.8–85.1
High p53 expression; No; %; 95% CI (cut-off 52%)	39; 30.9 23.5–39.5	12; 50% 31.4–68.6
CD44		
Number of evaluated cases	146	26
Mean ± SD; 95% CI	74.1 ± 27.8 69.6–78.7	13.5 ± 14.3 7.7–19.2

Table 2.1. continued

Variable	GBM	DA
Median; IQR	86.5; 36	8.5; 15
High CD44 expression; No; %; 95% CI (cut-off 50%)	119; 81.5 74.4–86.9	0; 0 0–12
CD44		
High CD44 expression; No; %; 95% CI (cut-off 86%)	75; 51.4 43.3–59.3	0; 0 0–12
High CD44 expression; No; %; 95% CI (cut-off 8%)	144; 98.6 95.1–99.6	14; 53.8 35.4–71.2
p21		
Number of evaluated cases	146	20
Mean ± SD; 95% CI	21.2 ± 15.0 18.7–23.6	6.9 ± 9.5 2.4–11.4
Median; IQR	19.0; 19	2.5; 7
High p21 expression; No; %; 95% CI (cut-off 20%)	72; 49.3 41.3–57.4	3; 15 5.2–36.0
High p21 expression; No; %; 95% CI (cut-off 2.5%)	145; 99.3 96.2–99.9	12; 60 38.6–78.1
p27		
Number of evaluated cases	113	23
Mean ± SD; 95% CI	69.7 ± 21.2 65.8–73.7	86.6 ± 11.6 81.6–91.7
Median; IQR	74; 31	92; 17
High p27 expression; No; %; 95% CI (cut-off 70%)	68; 60.1 50.9–68.7	20; 86.9 67.8–95.4
High p27 expression; No; %; 95% CI (cut-off 92%)	11; 9.7 5.2–17.1	12; 52.2 32.9–70.7
PDGFRA		
Number of evaluated cases	146	20
Mean ± SD; 95% CI	7.9 ± 17.3 5.0–10.7	42.3 ± 35.5 25.7–59.0
Median; IQR	1.0; 4	42.0; 68
0–10 % of PDGFRA positive cells; No; %; 95% CI	118; 80.8 74.4–87.2	5; 26.3 6.5–46.1
10–50 % of PDGFRA positive cells; No; % 95% CI	19; 13.0 7.5–18.5	4; 21.1 2.7–39.4

Table 2.1. (end)

Variable	GBM	DA
> 50% of PDGFRA positive cells; No; % 95% CI	9; 6.2 2.3–10.1	10; 52.6 30.1–75.0
High PDGFRA expression; No; %; 95% CI (cut-off 50%)	9; 6.1 3.2–11.3	10; 50 29.9–70.1
High PDGFRA expression; No; %; 95% CI (cut-off 1%)	130; 89.0 82.9–93.1	20;100 83.9–100
PDGFRA		
High PDGFRA expression; No; %; 95% CI (cut-off 42%)	9; 6.2 3.2–11.2	10; 50 29.9–70.1
IDH1 R132H status		
Number of evaluated cases	146	26
Negative (Nr of cases; %; 95% CI)	141; 96.6 93.7–99.5	6; 23.1 6.9–39.3
Positive (Nr of cases; %; 95% CI)	5; 3.4 0.5–6.3	20; 76.9 60.7–93.1
MVD (CD34)		
Number of evaluated cases	107	23
Mean ± SD; 95% CI	40.7 ± 25.4 35.8–45.6	18.1 ± 12.1 12.9–23.3
Median; IQR	35.0; 29	13.0; 16
High MVD; Number of cases; %; 95% CI (cut-off 35%)	55; 51.4 42.0–60.7	3;1 3.0 4.5–32.1
High MVD; Number of cases; %; 95% CI (cut-off 13%)	98; 91.6 84.8–95.5	13; 56.5 36.8–74.4

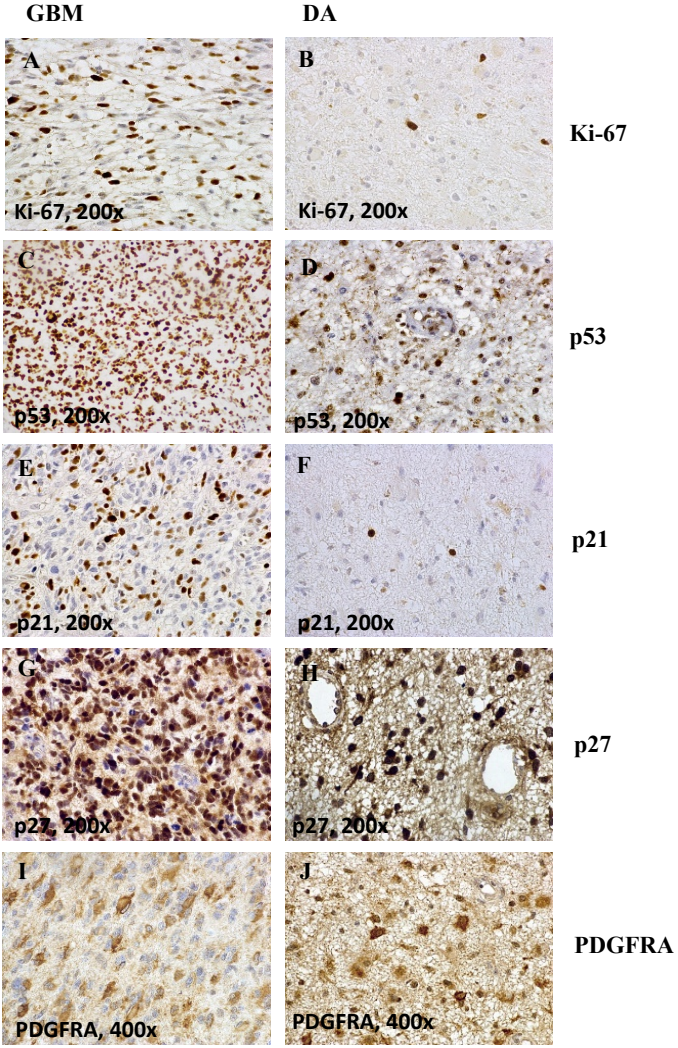

Figure 2.3. **IHC of evaluated markers in GBMs and Das**
A and B, Ki-67 proliferation fraction (PF): markedly increased PF in GBM (A) and low PF in DAs (B). C and D, nuclear expression of p53 protein: C, in GBM; D, in DA. E and F, nuclear expression of p21 protein: E, in GBM; F, in DA. G and H, nuclear expression of p27 protein: G, in GBM; H, in DA. I and J, cytoplasmic expression of PDGFRA: I, in GBM; J, in DA.

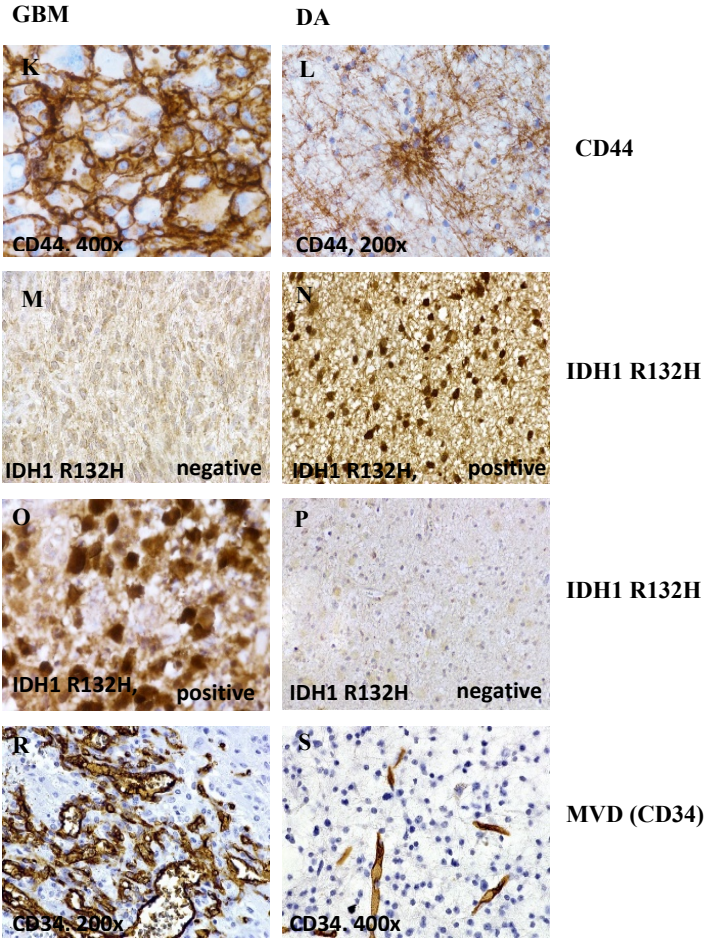

Figure 2.3. (continued) **IHC of evaluated markers in GBMs and DAs**
K and L, expression of CD44: K, in GBM, note intense, membranous expression; L, in DA, very weak expression in fibrillary processes of neoplastic cells, as well as more intense expression (arrow). M–P, status IDH1 R132H mutation by IDH1 R132H IHC: M, IDH1 R132H negative or primary GBM; O, IDH1 R132H positive or secondary GBM; N, IDH1 R132H positive DA; P, IDH1 R132H negative DA. K and S, evaluation of MVD by CD34: K, in GBM; S, in DA

2.4. Associations and correlations between clinical and immunohistochemical variables

2.4.1. Characteristics of GBM cases

No significant associations were found between patient age and any of the evaluated markers, although there was a tendency towards a younger age in secondary (IDH1 R132H positive) GBMs (Mann-Whitney U test, $z = -1.632$; $p = 0.060$).

A significant difference was found between gender and the expression of CD44 protein in GBMs. Thus, significantly higher expression of CD44 was found in females, according to the Mann-Whitney test ($z = -2.224$; $p = 0.026$) (Figure 3.20). CD44 also showed a weak, significant, negative correlation with GBM size ($r_s = -0.314$; $p < 0.0001$). In addition, higher CD44 expression values were more frequently found in GBMs of a smaller size (< 4 cm) (Mann-Whitney U test, $z = -2.364$; $p = 0.018$). Immunohistochemical visualization of CD44 expression is shown in Figure 2.4.

There was a trend towards lower Ki-67 labelling indices in GBMs in males (Mann-Whitney U test, $z = -1.913$; $p = 0.056$). There was also a weak but statistically significant correlation between Ki-67 and maximum diameter in GBMs ($r_s = 0.243$; $p = 0.013$). Immunohistochemical visualization of Ki-67 expression is shown in Figure 2.5.

p21 protein expression showed a very weak but significant negative correlation with maximum diameter in GBMs ($r_s = -0.181$; $p = 0.045$). A higher p21 protein expression was also observed in GBMs of a smaller size (< 4 cm) with the Mann-Whitney U test ($z = -2.460$; $p = 0.014$).

p27 protein expression showed a significant difference between gender and multifocality in GBMs. Thus, a higher expression of p27 was observed in males (Mann-Whitney U test; $z = -2.174$; $p = 0.030$) and multifocal GBMs

(Mann-Whitney U test; z =−2.1; p=0.037). Immunohistochemical visualization of p27 expression is shown in Figure 2.6.

Mean ranks of PDGFRA expression tended toward higher expression in multifocal GBMs (mean ranks: 92.34 versus 71.18) (Mann-Whitney U test; z = −1.9; p = 0.049). Immunohistochemical visualization of PDGFRA expression is shown in Figure 2.7.

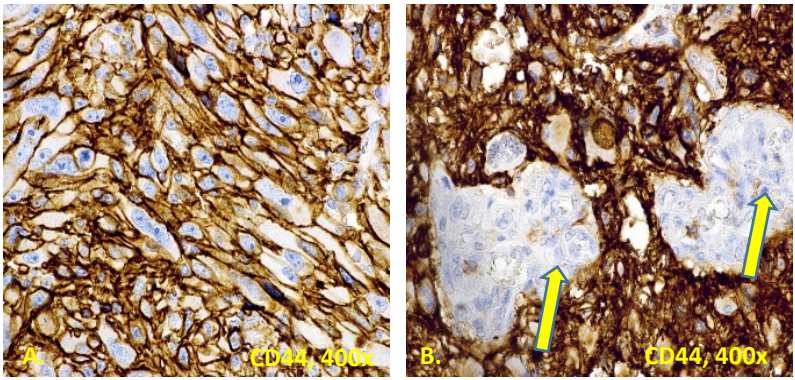

Figure 2.4. **Intense membranous expression of CD44 in GBM**
Note prominent, proliferative blood vessels negative for CD44 (internal negative control) (arrows). Immunoperoxidase, anti-CD44, original magnification 400×.

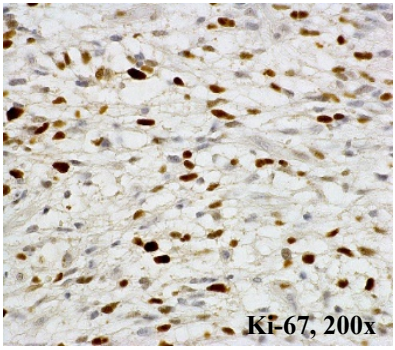

Figure 2.5. **Ki-67 proliferation fraction in GBM**
Immunoperoxidase, MIB-1, original magnification 200×.

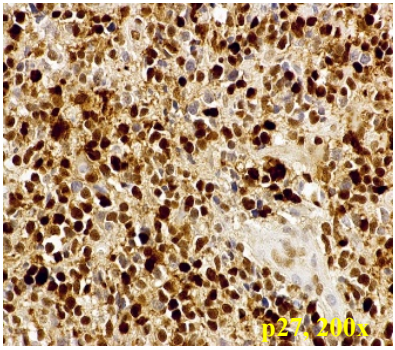

Figure 2.6. **Nuclear expression of p27 in GBM**
Immunoperoxidase, anti-p27, original magnification 200×.

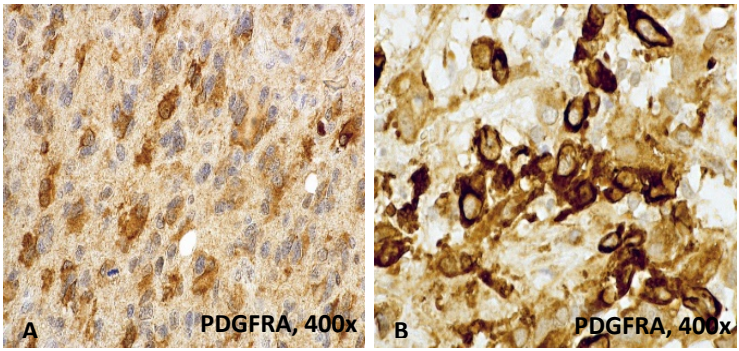

Figure 2.7. **Membranous and cytoplasmic expression of PDGFRA in GBM**
Immunoperoxidase, anti-PDGFRA, original magnification 400×.

2.4.2. Characteristics of DA cases

There was a statistically significant gender difference in mean ranks of Ki-67 expression in DAs. Thus, the mean rank of Ki-67 expression was statistically significantly higher in males (mean rank = 16.8) than in females (mean rank = 9.3) in DAs (Mann-Whitney U test, z = -2.201; p = 0.010).

There was a moderate, positive correlation of p27 with age (rs = 0.519; p = 0.011). Immunohistochemical visualization of the Ki-67 proliferation fraction and p27 expression is shown in Figures 2.8 and 2.9.

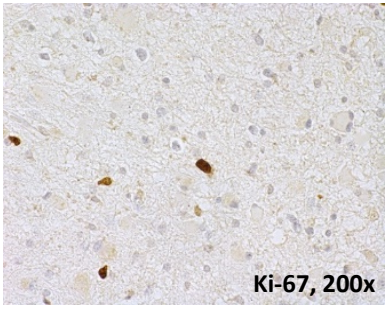

Figure 2.8. **Ki-67 proliferation fraction in DA, MIB-1, original magnification 400×.**

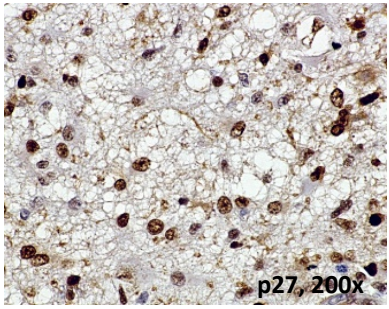

Figure 2.9. **Nuclear p27 expression in DA, anti-p27, original magnification 400×.**

2.5. Associations and correlations between immunohistochemical variables

2.5.1. Characteristics of GBM cases

In GBMs, very weak positive correlations between p53 and the proliferation fraction by Ki-67 (rs = 0.196; p = 0.027) and PDGFRA (rs = 0.181; p = 0.043) were found. A weak positive correlation between p53 and MVD was found (rs = 0.228; p = 0.031). Ki-67 tended toward a very weak, negative correlation with p27 (rs = 0.199; p = 0.055). Mean ranks of p53 expression were significantly higher in secondary GBMs (IDH1 R132H positive) (Mann-Whitney U test, z = -3.555; p = 0.0001).

The full results of correlations and associations between IHC markers in GBMs are summarized in Table 2.2.

Table 2.2.

The correlations and associations between IHC markers in GBMs by Spearman's rank order correlation and Mann-Whitney U test

Variables	Ki-67	p53	CD44	PDGFRA	p21	p27	MVD
Ki-67	NP	**0.196** **0.027**	-0.162 0.070	0.098 0.274	-0.060 0.503	**-0.199** **0.055**	-0.038 0.723
p53	**0.196** **0.027**	NP	-0.073 0.414	**0.181** **0.043**	0.019 0.829	0.037 0.725	**0.228** **0.031**
CD44	-0.162 0.070	-0.073 0.414	NP	-0.141 0.090	0.037 0.659	-0.144 0.128	0.038 0.694
PDGFRA	0.098 0.274	**0.181** **0.043**	-0.141 0.090	NP	-0.152 0.067	-0.056 0.555	0.132 0.176
p21	-0.060 0.503	0.019 0.829	0.037 0.659	-0.152 0.067	NP	0.119 0.211	-0.054 0.580
p27	**-0.199** **0.055**	0.037 0.725	-0.144 0.128	-0.056 0.555	0.119 0.211	NP	-0.121 0.214
MVB	-0.038 0.723	**-0.228** **0.031**	0.038 0.694	0.132 0.176	-0.054 0.580	-0.121 0.214	NP
IDH1 R132H	-0.656 0.512	**-3.555** **0.0001**	-1.201 0.230	-0.449 0.654	-1.545 0.122	-1.632 0.103	-1.281 0.200

* r_s, z and p values are shown in the table. Statistically significant correlations ($p < 0.05$) are marked in bold.
* Abbreviations in the table: NA, not applicable; MVD, microvascular density; PDGFRA, platelet-derived growth factor receptor alpha; IDH1, isocitrate dehydrogenase 1

2.5.2. Characteristics of DA cases

In DAs, there was a significant, moderate, positive correlation between PDGFRA and p53 ($r_s = 0.544$; $p = 0.013$). In contrast, the correlation between PDGFRA and CD44 was negative, again reaching moderate strength ($r_s = -0.592$; $p = 0.006$).

There was a strong, negative correlation between PDGFRA and p21 in DAs ($r_s = -0.603$; $p = 0.008$). A moderate, negative correlation was also found between PDGFRA and MVD ($r_s = -0.501$; $p = 0.034$). p21 had a positive, moderate correlation with MVD in DAs ($r_s = 0.458$; $p = 0.049$). The full results of correlations between IHC markers in DAs are summarized in Table 2.3. Immunohistochemical visualization of CD44, PDGFRA expression and MVD is shown in Figures 2.10, 2.11 and 2.12.

Table 2.3.

The correlations between IHC markers in DAs by Spearman's rank order correlation Mann-Whitney U test

Variables	Ki-67	p53	CD44	PDGFRA	p21	p27	MVD
Ki-67	NP	0.339 0.106	-0.130 0.544	-0.002 0.992	0.146 0.551	0.276 0.226	0.215 0.350
p53	0.339 0.106	NP	-0.382 0.066	**0.544** **0.013**	-0.260 0.282	0.149 0.518	0.274 0.230
CD44	-0.130 0.544	-0.382 0.066	NP	**-0.592** **0.006**	0.170 0.474	0.302 0.162	**0.490** **0.018**
PDGFRA	-0.002 0.992	**0.544** **0.013**	**-0.592** **0.006**	NP	**-0.603** **0.008**	0.149 0.555	**-0.501** **0.034**
p21	0.146 0.551	-0.260 0.282	0.170 0.474	**-0.603** **0.008**	NP	-0.290 0.229	**0.458** **0.049**
p27	0.276 0.226	0.149 0.518	0.302 0.162	0.149 0.555	-0.290 0.229	NP	0.204 0.350
MVD	0.215 0.350	-0.274 0.230	**0.490** **0.018**	**-0.501** **0.034**	**0.458** **0.049**	0.204 0.350	NP

* r_s, z and p values are shown in the table. Statistically significant correlations ($p < 0.05$) are marked in bold.
* Abbreviations in the table: NA, not applicable; MVD, microvascular density; PDGFRA, platelet-derived growth factor receptor alpha; IDH1, isocitrate dehydrogenase 1

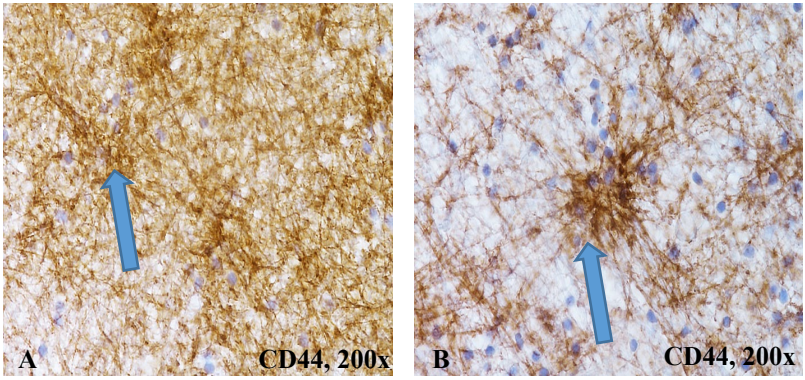

Figure 2.10. **Expression of CD44 in DAs**
Weak background expression in fibrillary cytoplasmic processes of astrocytes is seen together with foci of higher expression intensity (arrows). Immunoperoxidase, anti-CD44, original magnification 200×.

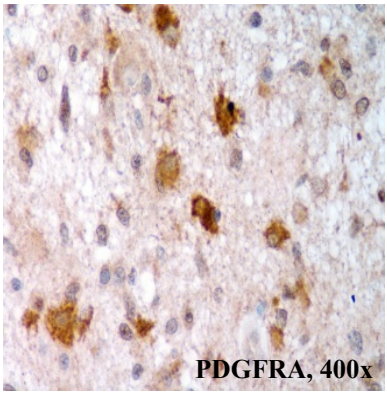

Figure 2.11. **Cytoplasmic expression of PDGFRA in DA**
Immunoperoxidase, anti-PDGFRA, original magnification. 400×

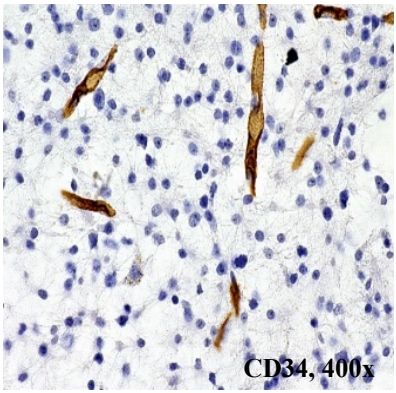

Figure. 2.12. **Microvessels in DA**
Immunoperoxidase, anti-CD34, original magnification 400×.

2.6. Survival

2.6.1. Characteristics of GBM cases

The survival data was available for 135 patients, which have been included in survival analysis. At the end of the study, 2/135 (1.5%; 95% CI = 0–5.2) patients were alive, but 133/135 (98.5%; 95% CI = 94.8–99.6) had died during the observation period. The overall median survival time was 7.9 months (95% CI = 6.8–9.0). The survival plot by Kaplan-Meier is shown in Figure 2.13.

Within the first month after their surgical operation, 6/135 (4.5%; 95% CI = 2.0–9.3) patients had died, but 129/135 (95.5%; 95% CI = 90.6–97.9) were alive. Six months after their operation 53/135 (39.3%; 95% CI = 31.4–47.7) patients had died. One year after their operation 86/135 (63.7%; 95% CI = 55.3–71.3) patients had died. Two years after their operation 122/135 (90.4%; 95% CI = 84.2–94.3) patients had died. Three years after their operation 133/135 (98.5%; 95% CI = 94.8–99.6) patients had died.

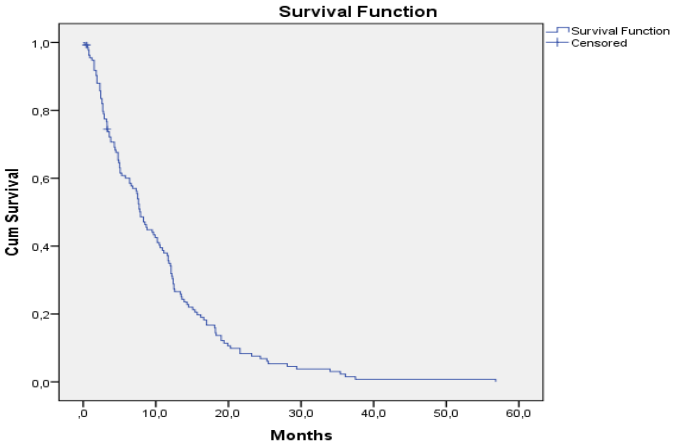

Figure 2.13. **Kaplan-Meier survival plot of patients with GBMs**

2.6.2. Characteristics of DA cases

The survival data was available for 25 patients that have been included in survival analysis. At the end of the study 14/25 (56.0%; 95% CI = 37.0–73.3) patients were alive, but 11/25 (44.0%; 95% CI = 26.6–62.9) had died during the observation period. Because of the small study group and small number of death cases, statistical calculations are embarrassing and the overall median survival time could not be calculated. The survival plot by Kaplan-Meier is shown in Figure 2.14. As can be seen from the plot, the survival curve does not drop below 0.5.

Within the first year after their surgical operation all patients were alive (25/25). Two years after their operation 3/25 (12%; 95% CI = 4.2–29.9) patients had died, but 22/25 (88%; 95% CI = 70.0–95.8) were alive. Three years after their operation 5/25 (20%; 95% CI = 8.8–39.1) patients had died, but 20/25 (80%; 95% CI = 60.9–91.1) were alive.

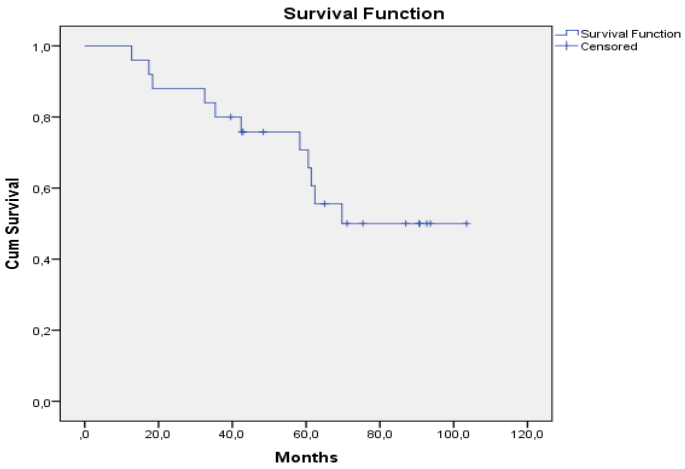

Figure 2.14. **Kaplan-Meier survival plot of patients with DAs**

2.7. Associations between survival and clinical variables

2.7.1. Prognostic characteristics of GBMs

There was a statistically significant difference in overall survival (OS) regarding patient age (log-rank, $p < 0.001$). The median OS of patients ≤ 65 years old was 11.7 (95% CI = 8.1–15.3) months, however the median OS of patients older than 65 years was 5 (95% CI = 3.2–6.8) months. Thus, younger age at diagnosis is associated with a significantly higher survival rate in GBM patients (Figure 2.15).

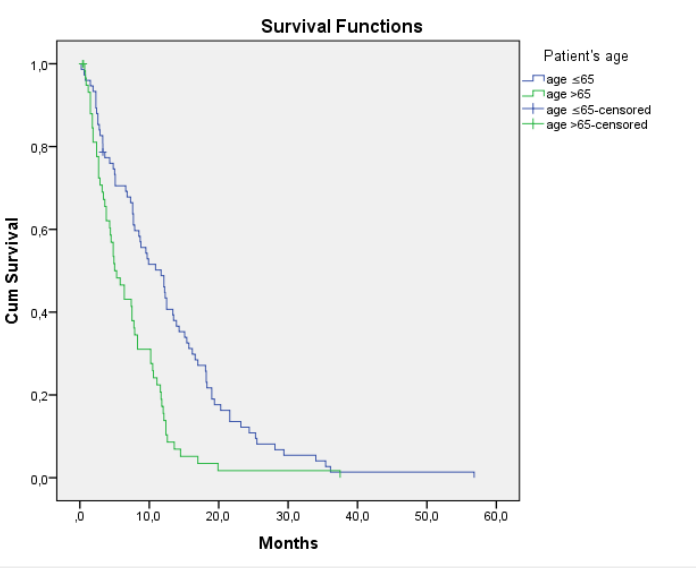

Figure 2.15. **Kaplan-Meier survival curves by patient age in patients with**

There was a statistically significant difference in median OS regarding tumour localization (log-rank, $p = 0.018$). GBMs localized in occipital lobes were excluded from survival analysis because of the rarity of cases (n=2). There was a tendency toward higher survival rates in GBMs localized in parietal lobes over frontal localization ($p = 0.06$). GBMs located in multiple lobes also had a worse prognosis. The median OS rates in patients with tumours localized in

frontal, temporal and parietal lobes were 8.3 (95% CI = 6.7–9.8) months, 7.7 (95% CI = 4.0–11.4) months and 12.6 (95% CI = 10.4–14.8) months. In comparison, the median survival of patients with tumours involving more than one lobe was 6.4 (95% CI = 3.7–9.0) months. The corresponding Kaplan-Meier curves are shown in Figure 2.16.

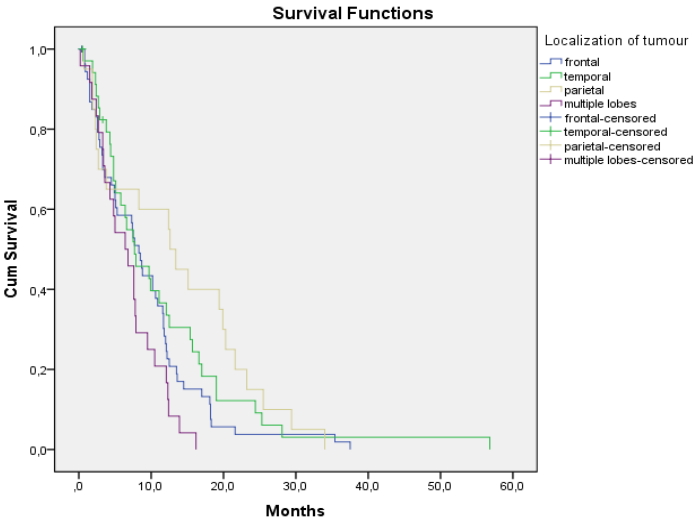

Figure 2.16. **Kaplan-Meier survival curves by localization of tumour in patients with GBMs**

There was a statistically significant difference in median OS regarding tumour size (log-rank, p = 0.018). Median OS rates in patients with tumours ≤ 4 cm and > 4 cm were, respectively, 11.8 (95% CI = 8.1–15.5) months and 6.8 (95% CI = 4.7–8.8) months. The corresponding Kaplan-Meier curves are shown in Figure 2.17.

Patients diagnosed with multifocal GBMs had significantly worse survival than those with solitary tumours (log-rank, p = 0.002). The median OS survival in patients with multifocal GBMs was 3.4 (95% CI = 0–6.9) months compared with a median OS of 8.7 (95% CI = 6.8–10.6) months in patients with

solitary tumours. The corresponding Kaplan-Meier curves are shown in Figure 2.18.

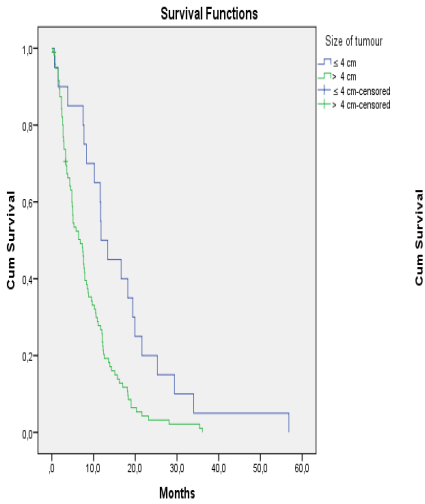

Figure 2.17. **Kaplan-Meier survival curves by size of tumour in patients with GBMs**

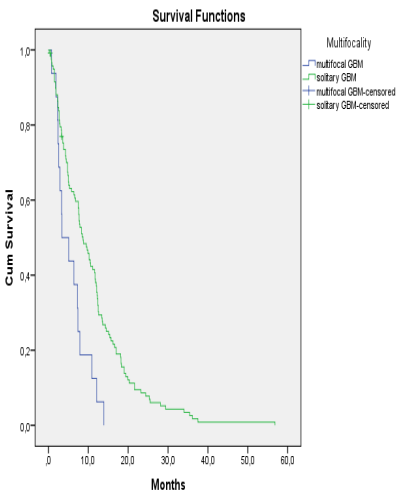

Figure 2.18. **Kaplan-Meier survival curves by multifocal versus solitary tumours in patients with GBMs**

A significant difference in median OS was observed in GBMs by type of treatment (log-rank, $p < 0.001$). Thus, tumours treated with the current standard of care by surgery followed by radiotherapy and chemotherapy with temozolomide had a median OS of 12.1 (95% CI = 11.2–13.0) months, versus surgery plus radiotherapy – 7.5 (95% CI = 5.4–9.6) months, versus surgery only – 2.9 months (95% CI = 1.4–4.4). The corresponding Kaplan-Meier curves are shown in Figure 2.19.

There were no statistically significant survival differences in median OS by gender ($p = 0.560$).

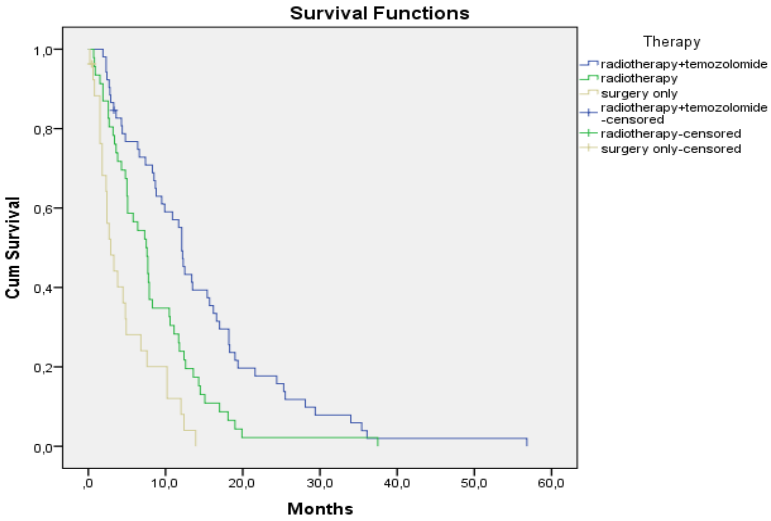

Figure 2.19. **Kaplan-Meier survival curves by therapy in patients with GBMs**

2.7.2. Prognostic characteristics of DAs

In DAs, there was a statistically significant difference in survival regarding gender (log-rank, p = 0.002). Females showed better survival than males, as can be seen in Figure 2.20. At the end of the study 11/13 (84.6%; 95% CI = 57.8% – 95.7%) females and only 3/12 (25%; 95% CI = 8.9% – 57.2%) males were alive. The median OS of males with DAs was 58.3 (95% CI = 31.1–85) months. The median OS in females cannot be calculated because of the few death cases (n = 2) and small study group.

There were no statistically significant survival differences by localization (p = 0.812) in patients with DAs.

All DAs were large tumours whose size exceeded 4 cm, thus tumour size was not included in survival analysis.

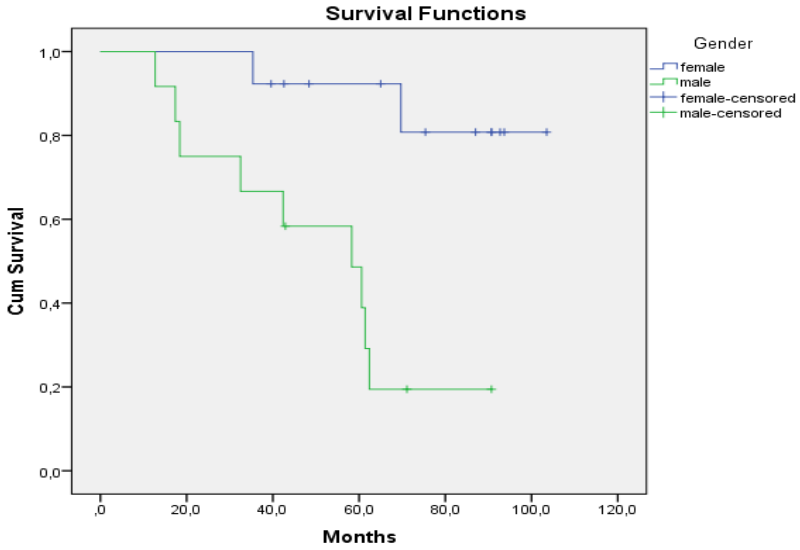

Figure 2.20. **Kaplan-Meier survival curves by gender in patients with DAs**

2.8. Associations between survival and immunohistochemical variables

2.8.1. Immunohistochemical prognostic markers in GBMs

In GBMs, a statistically significant survival difference was found in patients regarding IDH1 R132H mutant protein expression (log-rank, $p = 0.040$). Thus, patients with secondary GBMs (IDH1 R132 positive) had a median OS of 18.3 (95% CI = 18.0–18.5) months versus 7.7 (95% CI = 6.3–9.0) months in patients with primary GBMs (IDH1 R132H negative). The corresponding Kaplan-Meier curves are shown in Figure 2.21.

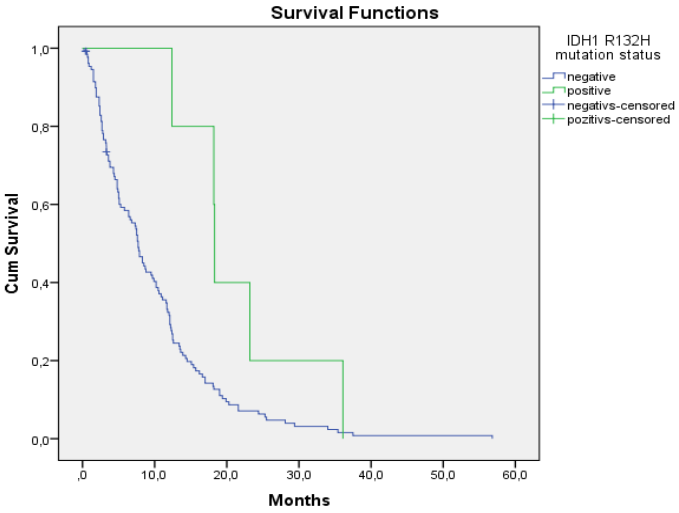

Figure 2.21. **Kaplan-Meier survival curves by IDH1 R132H mutation status in patients with GBMs**

A trend towards a difference in OS was found in patients with GBMs by PDGFRA expression at a cut-off point of 50% (log-rank, p = 0.066). The median OS of patients with high PDGFRA expression was 6.4 (95% CI = 2.8–9.9) months versus 8.3 (6.4–10.1) months in patients with low PDGFRA expression. The corresponding Kaplan-Meier curves are shown in Figure 2.22.

The proliferation index by Ki-67 showed a statistically non-significant difference with survival (log-rank, p = 0.252). However, using a cut-off of 25% by visual inspection survival curves are different, so the curves overlap in the first five months but diverge thereafter and then cross again after 20 months of follow-up. The median survival of patients with high Ki-67 proliferation indices was 7.4 (95% CI = 5.7–9.1) months versus 13.5 (95% CI = 9.1–17.8) months in

patients with low Ki-67 proliferation indices. The corresponding Kaplan-Meier curves are shown in Figure 2.23.

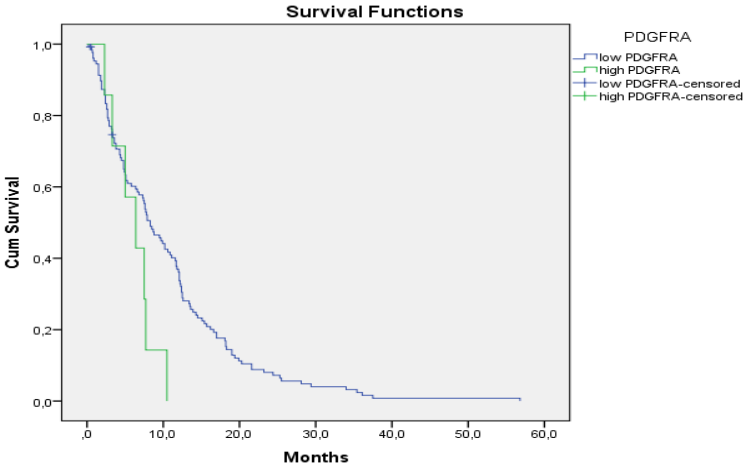

Figure 2.22. **Kaplan-Meier survival curves by PDGFRA expression in patients with GBMs** (cut-off value – 50%)

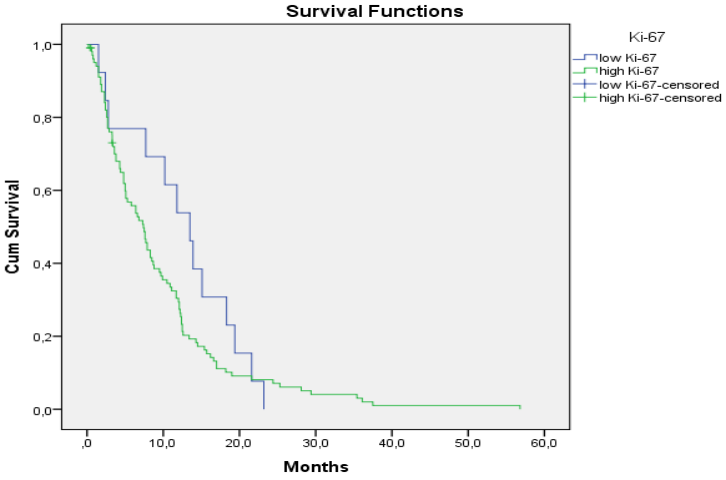

Figure 2.23. **Kaplan-Meier survival curves by Ki-67 expression in patients with GBMs** (cut-off value – 25%)

2.8.2. Immunohistochemical prognostic markers in DAs

In DAs, a statistically significant survival difference was found in patients regarding Ki-67 expression using a cut-off of 5.5% (log-rank, p = 0.037). High Ki-67 proliferation indices (≥ 5.5%) were present in 12/23 (52.2%; 95% CI = 33.0–70.8) DA cases. Low Ki-67 proliferation indices (< 5.%) were present in 11/23 (47.8%; 95% CI = 29.2–67.0) DA cases. At the end of the study 7/12 (58.3%; 95% CI = 31.9–80.7) patients had died within the tumour group with high Ki-67 proliferation indices compared with 2/11 (18.2%; 95% CI = 5.1–47.7) patients that had died in the tumour group with low Ki-67 proliferation indices. The median OS in patients with high Ki-67 expression was 60.6 months (95% CI = 35.3–85.9). The median OS in patients with low Ki-67 expression could not be calculated because of the few cases of death and small study group. The corresponding Kaplan-Meier curves are shown in Figure 2.24.

A statistically significant survival difference was found in patients regarding PDGFRA expression using a cut-off of 50% (log-rank, p = 0.017). High PDGFRA expression (≥ 50%) was present in 10/19 (52.6%; 95% CI = 31.7–72.6) DA cases. Low PDGFRA expression (< 50%) was present in 9/19 (47.3%; 95% CI = 27.3–68.3) DA cases. At the end of the study 1/10 (10%; 95% CI = 1.8–40.4) of the patients had died within the tumour group with high PDGFRA expression compared with 5/9 (55.6%; 95% CI = 26.7–81.1) patients that had died in the tumour group with low PDGFRA expression. The median OS in patients with low PDGFRA expression was 61.4 months (95% CI = 9.9–112.0). The median OS in patients with high PDGFRA expression could not be calculated because of the few cases of death and small study group.

The corresponding Kaplan-Meier curves are shown in Figure 2.25.

As regards other immunohistochemical markers, no significant survival differences were found.

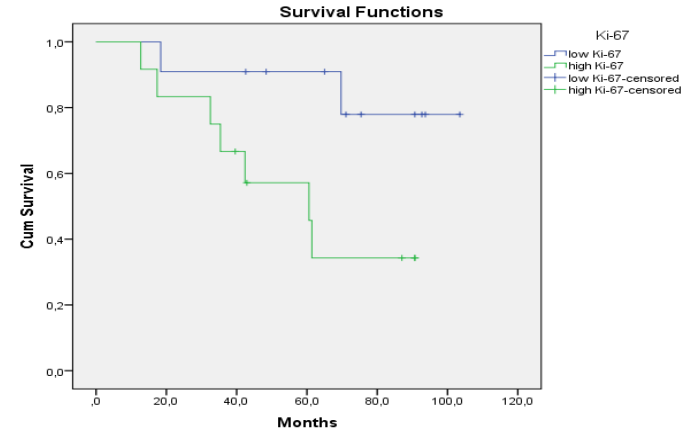

Figure. 2.24. **Kaplan-Meier survival curves by Ki-67 expression in patients with DAs** (cut-off value – 5.5%)

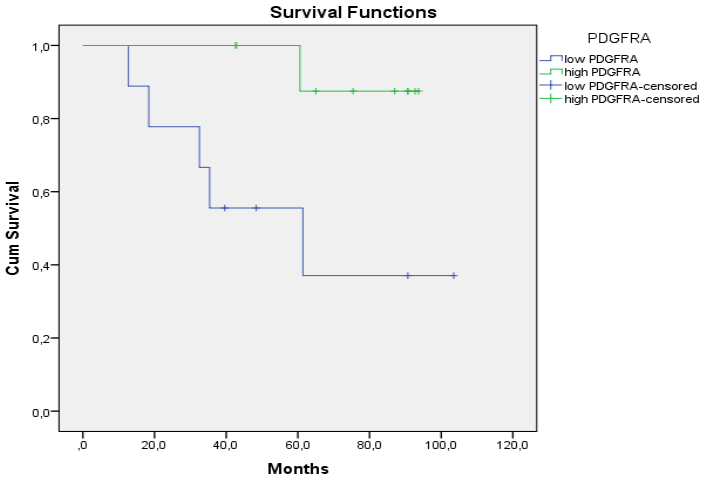

Figure 2.25. **Kaplan-Meier survival curves by PDGFRA expression in patients with DAs** (cut-off value – 50%)

2.9. Immunohistochemical subtypes and survival

The immunohistochemical data of p53, IDH1 R132H, PDGFRA and CD44 expression was used to determine the subtype of GBMs (see Materials and Methods). Based on these protein expression signatures, three categories of GBMs were distinguished: proneural, mesenchymal and not otherwise classified, referred to as "Other". For subtyping of GBMs we used two different cut-off levels for immunohistochemical markers based on the literature studies and on the median value of expression.

2.9.1. Immunohistochemical subtypes of GBMs

The majority of GBM cases were of the proneural subtype – 73/146 (50.0%; 95% CI = 42.0–58.0), followed by other (not otherwise classified) – 46/146 (31.5%; 95% CI = 24.5–39.4) and the mesenchymal subtype – 27/146 (18.5%; 95% CI = 13.0–25.6).

There were no associations between subtypes of GBMs and any clinical or immunohistochemical parameters (Ki-67, MVD, p21, p27). There was no difference in OS between subtypes of GBMs (log-rank, p value = 0.424) (Figure 2.26A).

Furthermore, a response of therapy was evaluated on survival in different GBM subtypes.

As shown in Figure 3.51B, in the proneural subtype there was a tendency for the addition of temozolomide to improve OS compared with radiotherapy alone (p = 0.061) (the median OS ratio was 1.6). However, the visual tendency towards a difference between Kaplan-Meier curves was more perspicuous. Radiotherapy also improved OS in the proneural subtype compared with surgery only (p = 0.008).

In the mesenchymal subtype, the addition of temozolomide significantly improved OS compared with radiotherapy alone (p = 0.002). However, addition

of radiotherapy did not improve the OS of the patients with the mesenchymal subtype compared with surgery only (p = 0.857) (Figure 3.51C). Thus, the addition of radiotherapy did not have any benefit compared with surgery only in patients with the mesenchymal subtype.

In other GBMs (not otherwise classified), there was a statistically significant OS difference only between those GBMs treated with adjuvant chemotherapy and radiotherapy and those only treated surgically (p = 0.031). There were no statistically significant differences between other groups: temozolomide + radiotherapy versus radiotherapy alone (p = 0.319) and radiotherapy versus surgery only (p = 0.080) (Figure 3.51D)

The corresponding Kaplan-Meier curves are shown in Figure 2.26. The median OS rates for GBM subtypes, as well as the number of cases and p values for pairwise comparisons, are summarized in Table 2.4.

In addition to previously described subtypes, cut-off levels based on median expression values of immunohistochemical markers were also used for subtyping of GBMs.

According to cut-off levels based on median expression, the proportion of GBMs of the proneural subtype had increased – 95/146 (65.1%; 95% CI = 57.0–72.3), followed by other (not otherwise classified) – 32/146 (21.9%; 95% CI = 15.9–29.3) and the mesenchymal subtype – 19/146 (13.0%; 95% CI = 8.5–19.4).

No associations were found between subtypes of GBMs and any clinical or immunohistochemical parameters (Ki-67, MVD, p21, p27). There was no difference in OS between subtypes of GBMs (log-rank, p value = 0.511).

When the response to treatment is evaluated in GBM subtypes (based on cut-offs from median values), Kaplan-Meier survival lines show a very similar shape and abruptness of lines between survival plots, analogous to previously described GBM subtypes that were based on cut-offs from the literature studies.

Table 2.4.

Median OS rates in GBM subtypes together with p values for pairwise comparisons

Subtype (n = 135*)	**Therapy** (n = 135*)	**Median OS**	**95% CI**	**p values**		
Proneural (n = 66)	TMZ + radiotherapy (n = 25)	12.3	8.4–16.2	0.061		< 0.001
	Radiotherapy (n = 27)	7.6	7.1–8.1		0.008	
	Surgery only (n = 14)	2.4	1.1–3.6			
Mesenchymal (n = 26)	TMZ + radiotherapy (n = 11)	11.7	6.4–16.9	0.002		0.003
	Radiotherapy (n = 9)	2.7	0.3–5.0		0.857	
	Surgery only (n = 6)	2.7	2.0–3.3			
Other (n = 43)	TMZ + radiotherapy (n = 20)	12.2	6.7–17.6	0.319		0.031
	Radiotherapy (n = 14)	8.3	3.7–12.9		0.080	
	Surgery only (n = 9)	4.9	3.9–5.9			

* Data about the therapy were missing in 11 cases. Thus, 135 cases of GBMs were available for this analysis.

* Abbreviations in the table: OS, overall survival; TMZ, temozolomide; CI, confidence interv

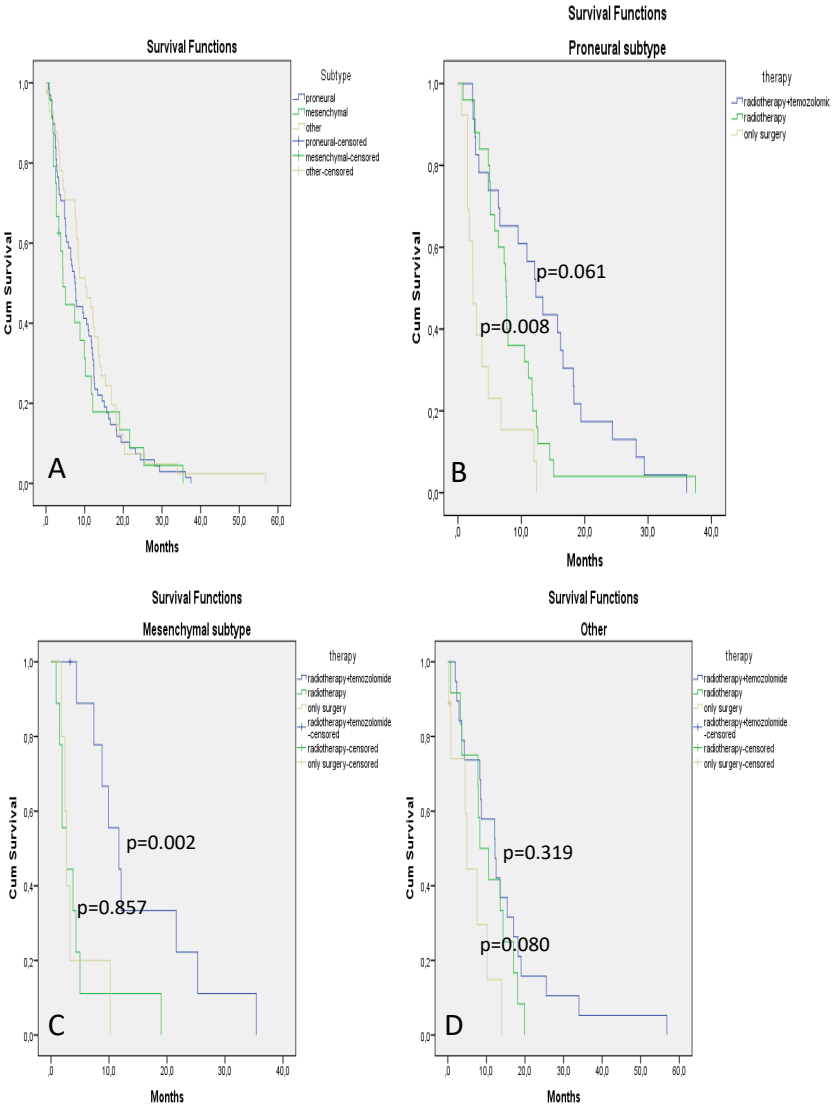

Figure 2.26. **Kaplan-Meier survival curves by GBM subtype and treatment type**

2.9.2. Immunohistochemical subtypes of DAs

Using both cut-off values, most DAs belong to the proneural subtype 24/26 (92.3%; 95% CI = 75.8–97.9), while the remaining 2/26 (7.6%; 95% CI = 2.1% – 24.1%) DAs were not otherwise classified (“other”) according to cut-off values based on the literature studies. CD44 expression in all DAs was very low, according to the literature-defined cut-off of 50%, and CD44 expression reached this level in only one tumour. Because of the few cases and the predominance of proneural signature survival analysis by subtype and therapy was not performed.

3. Discussion

Diffuse gliomas do not rank among malignancies with the highest incidence such as lung cancer, breast cancer or colorectal cancer, but, nevertheless, gliomas rank among the most aggressive human malignancies and have limited treatment options. The most common and the most aggressive type of glioma is GBM, so many international studies have researched this tumour. It is crucial to better understand specific signalling pathways and molecular alterations determining biological features of gliomas, such as invasion, proliferation and resistance to current therapy, because this is the only thing that can bring a ray of hope of improved target-specific management, as well as the development of personalized therapy. The current standard therapy, which includes chemotherapy with temozolomide and radiotherapy followed by surgery, is the best available treatment nowadays, but prognosis is still very bad (Stupp *et al.*, 2014, 2005). Fortunately, over the last 10 years, huge scientific progress has been made in the field of molecular biology of gliomas, creating a completely new understanding of these fatal tumours. One such breakthrough was complete sequencing of GBM whole genomes in a large group of patients with GBMs by the TCGA project (Cancer Genome Atlas Research, 2008). Due to comprehensive high-throughput analysis of GBM genome, better characterization of the genomic landscape of glioma was possible and several critical pathogenesis-driven mutations were identified in such genes, such as IDH1 and IDH2, EGFR, PDGFRA, ATRX and others (Brennan *et al.*, 2013; Parsons *et al.*, 2008; Verhaak *et al.*, 2010; Yan *et al.*, 2009).

It was also found that GBMs are not single entities as previously thought, but are rather composed of molecularly and biologically distinct subsets of the tumours, albeit with the same morphological appearance. Several studies have been performed to identify subtypes of gliomas based on molecular and proteomic signatures (Motomura *et al.*, 2012; Parsons *et al.*, 2008; Verhaak *et*

al., 2010). For example, Verhaak *et al.* described four glioblastoma molecular subtypes based on gene expression analysis – classical, proneural, mesenchymal and neural (Verhaak *et al.*, 2010). The tumours that possess similar molecular signatures and expression patterns likely share a common pathogenesis, reflecting similar therapy responses and prognoses.

Some of these identified genomic and proteomic signatures can potentially be used to develop new molecularly targeted therapies; in addition, they can be used as prognostic or predictive factors that provide some clues for a more personalized treatment approach.

Molecular profiling of gliomas is a time-consuming, very expensive technique that also requires unfixed tumour tissues. For the practical needs in routine, analysis of prognostic factors needs to be cheaper and easy to replicate, thus immunohistochemistry could be a good surrogate for other more expensive methods. Recent molecular advantages in the wider implementation of immunohistochemistry in glioma profiling and new immunohistochemical markers have been developed for routine use, such as IDH1 132H.

There have been several attempts at immunohistochemistry-based molecular subtyping of gliomas (Le Mercier *et al.*, 2012; Popova *et al.*, 2014; Trabelsi *et al.*, 2016).

Within this study we used IHC to assess the expression of some of the proteins that have been reported to have a prognostic importance or determine basic biological features of malignant tumours, such as invasion, regulation of cell cycle and proliferation. Inspired by the molecular classification of gliomas described by Verhaak *et al.*, we also tried to subdivide GBMs into several molecular groups and assess their prognostic significance. In addition to immunohistochemistry, the prognostic impact of clinical parameters and possible correlations between any of the examined parameters was assessed.

3.1. Overall survival and treatment

In this study, the median OS of all patients with GBM was 7.9 months (95% CI = 6.8–9.0), which is shorter than that described in other studies by different authors where the median OS ranged from 9.7 to 13.6 months (Back *et al.*, 2007; Johnson and O'Neill, 2012; Kumar *et al.*, 2013; Ulutin *et al.*, 2006). In this study there were only two (1.5%; 95% CI = 0–5.8) patients who survived more than three years. The longest survival in this study was 56 months, or 4.6 years. In the present study, the one- and two-year survival rates for patients with GBM were 36.3% and 9.6%, respectively. These survival rates are comparable to other studies, but on average are shorter than those published by the majority of researchers (Ahmadloo *et al.*, 2013; Ma *et al.*, 2009; Paszat *et al.*, 2001; Scoccianti *et al.*, 2010).

Patients with DAs had a significantly better prognosis than those with GBMs. In this study, the two- and three-year survival of patients with DAs was 88% and 80%, respectively. The median OS could not be calculated because of the small study group and short duration of follow-up time. Researchers from the USA (Mayo clinic) performed a large study on the survival of patients with diffuse gliomas with a median follow-up time of 13.6 years, and they reported a median OS of 6.9 years and 10-year survival rate of 36% (Schomas *et al.*, 2009). In this study, the median follow-up time of patients is 60.2 months, or 5.0 years. This is an adequate follow-up time for patients with GBMs who have a very poor prognosis. However, due to the relatively long survival time in patients with DAs, a longer duration of follow-up might be necessary for more precise survival time evaluation.

3.2. Clinical and morphological findings

Gender

In this study, both females and males were affected by GBMs and DAs in approximately equal proportions, so there were no gender differences in gliomas. In contrast to our study, a predominance of gliomas in males was reported in the literature, however in most studies gender differences are inconspicuous and the male:female ratio usually does not exceed 1.3 (Dobes *et al.*, 2011; Kushnir and Tzuk-Shina, 2011; Sun *et al.*, 2015). No differences in survival by gender were found in this study. Although various articles noted that male gender might be associated with better prognosis, multivariate analysis showed that women in the whole study group were older, and that may explain these survival differences (Tugcu *et al.*, 2010; Verger *et al.*, 2011).

Age

In this study, the mean (62.0 and 37.5 years) and median (62.0 and 35.0 years) age of GBMs and DAs was similar to those in other studies (Oszvald *et al.*, 2012; Schomas *et al.*, 2009; Schwartzbaum *et al.*, 2006). In our study, we have only five patients with secondary GBMs with a mean age of 50.6 years, which is slightly above the mean ages reported in the literature, but also the number of patients with secondary GBMs recruited in studies was higher (Juratli *et al.*, 2013; Ohgaki and Kleihues, 2007). In this study, older age was found to be associated with worse prognosis, which is supported by data from other publications (Buckner, 2003; Scott *et al.*, 2012).

Tumour localization

In the present study the most frequent location of GBM was the frontal lobe – 56/146 (38.4%; 95% CI = 30.5–46.3), followed by the temporal lobe – 41/146 (28.1%; 95% CI = 20.8–35.4). The data is comparable to other studies

where the frontal lobe was affected in 40% and 43% of cases and the temporal lobe in 28% and 29% of cases (Larjavaara *et al.*, 2007; Simpson *et al.*, 1993). With regard to DAs, in this study the most frequent localization is within frontal and temporal lobes – 13/26 (50%; 95% CI = 30.8–69.2) and 6/26 (23.1%; 95% CI = 6.9–39.3), respectively. This data also corresponds to other studies (Capelle *et al.*, 2013; Duffau and Capelle, 2004; Larjavaara *et al.*, 2007). In this study, multifocal involvement in GBM was identified in 11% of cases, very similar to other published articles where the frequency of multifocal gliomas was about 8–10 % (Barnard and Geddes, 1987; Djalilian *et al.*, 1999; Giannopoulos and Kyritsis, 2010).

Tumour size

As gliomas generally grow and invade brain parenchyma extensively before patients experience any symptoms, almost all gliomas are large tumours at the time of diagnosis. In this study most of the GBMs and all DAs were large tumours whose size exceeded 4 cm. Very few studies have described the relationship between glioma size and prognosis; some of these report that large tumour size is associated with a worse prognosis (Kashi *et al.*, 2015; Raysi Dehcordi *et al.*, 2012). In this study, patients with tumours of the largest size exceeding 4 cm had less favourable outcomes than those with smaller tumours.

Morphology

All GBMs in this study were diagnosed according to the 2016 WHO classification of CNS tumours and thus showed necrosis (ischaemic and/or pseudopalisading) and microvascular proliferation. Most of the GBMs in this study belong to typical or conventional morphology – 141/146 (96.6%; 95% CI = 93.7–99.5) and a minority of GBMs had giant-cell 2/146 (1.4%; 95% CI = 0–3.3) or gliosarcoma morphology – 3/146 (2.1%; 95% CI = 0–4.4).

The frequency of these rare GBM variants in our study were similar to that in other published reports where gliosarcomas and large-cell glioblastomas comprised 2–8 % and 1–5 % of cases, respectively (Castelli *et al.*, 2016; Kozak and Moody, 2009; Meis *et al.*, 1991; Valle-Folgueral *et al.*, 2008). In regard to five patients with immunohistochemically proven secondary GBMs (IDH1 R132H positive), only one GBM showed component of lower-grade glioma, thus confirming secondary GBM on morphological grounds. In addition, one other secondary GBM showed a focally increased number of gemistocytic astrocytes. The remaining three cases of secondary GBM did not differ from other conventional GBMs. In the literature some articles reported that secondary GBMs are characterized by a more frequent presence of gemistocytes, but this is not a reliable indicator of secondary origin (Reis *et al.*, 2001; Watanabe *et al.*, 1997). All 26 cases of DAs were diagnosed as diffuse fibrillary astrocytomas on morphological grounds according to the 2016 WHO classification of CNS tumours. All tumours in this study showed mild to moderate cellularity; individual tumour cells showed mild nuclear and cellular atypia, rare mitotic figures in some cases up to 2 mitoses per 10 high-power field were found.

3.3. Immunohistochemical profile of gliomas

Ki-67

The **Ki-67** proliferation index directly reflects the biological potential of the tumours and increasing values of Ki-67 strongly correlate with a higher grade of glioma (Arshad *et al.*, 2010; Johannessen and Torp, 2006; Skjulsvik *et al.*, 2014). Although the grading of gliomas is based on morphology but not on the proliferation fraction, Ki-67 can be used as a useful supplement to the histopathological diagnosis and grading of gliomas (Thotakura *et al.*, 2014). In our study there was a considerable difference in the proliferation rate between GBMs and DAs – 44.4% (95% CI = 41.1–47.6) versus 6.4% (95% CI = 4.7–8.0).

In this study, the mean value of the Ki-67 proliferation index in GBMs was relatively high – 44.4% (95% CI = 41.1–47.6) – compared to other studies that reported lower mean proliferation rates that ranged from 12% to 32% (Kleinschmidt-DeMasters *et al.*, 2005; Shivaprasad *et al.*, 2016; Wakimoto *et al.*, 1996). In DAs, Ki-67 was observed with a mean rate of 6.4% (95% CI = 4.7–8.0) and median of 5.5 (IQR = 6). In comparison, Norwegian authors reported mean and median Ki-67 proliferation rates in DAs of 5.2% and 4.5% with a range of 1% – 16% (Tove *et al.*, 2012).

The prognostic role of the Ki-67 proliferation index in GBMs remains inconclusive, with some studies showing a prognostic role (Ho *et al.*, 2003; Jin *et al.*, 2011) and others that did not find any significant association with prognosis (Moskowitz *et al.*, 2006; Yang *et al.*, 2013). However, in many survival studies researchers used different cut-off levels: 12.5%, 25% and 35% (Ho *et al.*, 2003; Jin *et al.*, 2011; Moskowitz *et al.*, 2006). However, using a cut-off of 25% by visual inspection, survival curves are different, but not statistically significantly so ($p = 0.252$).

In the current study, in DAs, Ki-67 was found to be a useful indicator of worse prognosis by using a cut-off of 5.5%. Other studies also support worse outcome in patients with DA harbouring a high Ki-67 proliferation fraction (Johannessen and Torp, 2006; Tove *et al.*, 2012). The Ki-67 proliferation fraction correlated with p53 protein expression ($rs = 0.196$; $p = 0.027$), which indicates oncogenic properties of p53 upregulating proliferation in neoplastic cells. Another cell cycle inhibitor, p27, tended towards an inverse correlation with Ki-67. Thus, loss of p27 and upregulation of p53 may be indicators of more proliferative features in GBMs. Interestingly, in DAs, the Ki-67 proliferation index also showed an association with patient gender, thus the mean ranks of Ki-67 expression were statistically significantly higher in males (mean rank = 16.8) than in females (mean rank = 9.4) in Das ($z = 2.563$; $p = 0.010$). Although

such an association between gender and proliferation fraction is poorly evaluated in glioma studies and the explanation is not clear, a growing number of studies have supported the role of sex hormones such as oestrogens, progesterone and androgens in a variety of brain tumours, including gliomas (Hartman *et al.*, 2009; Paruthiyil *et al.*, 2004; Sareddy *et al.*, 2016; Yu *et al.*, 2013). Recent studies especially emphasize the role of oestrogen receptor beta (ERβ), which is considered a tumour suppressor and is thus associated with inhibition of tumour proliferation. Downregulation of ERβ is associated with progression and a higher malignancy grade in many human cancers, including gliomas (Bardin *et al.*, 2004; Burns and Korach, 2012). However, the latest studies indicate that these gender differences cannot be explained by the hormones only, and the pathogenesis seems to be more complicated than previously thought. Thus, some recent studies have found several gender-different molecular, genome methylation and proteomic profiles of gliomas (Johansen *et al.*, 2020; Kfoury *et al.*, 2018; Yang *et al.*, 2019).

p53

Because p53 has a very short half-life time, it is present in cells at low levels under normal conditions and accumulation of p53 is a direct result of DNA damage, hypoxia or oncogene activation (Ashcroft and Vousden, 1999). In contrast to the wild-type p53 protein, which is quickly degraded within cells, mutations in the TP53 gene lead to overexpression of the more stable mutant p53 protein, which accumulates in the nucleus and can be detected immunohistochemically. In this study, 64.3% (95% CI = 55.6–72.1) of GBMs were positive for p53 protein using a cut-off value of 10%. Other authors, by using the same cut-off value, have found p53 expression values that ranged from 41 to 75 % (Kawasoe *et al.*, 2015; Popova *et al.*, 2014; Takano *et al.*, 2012). In this study, high p53 protein expression was found in 31.7% (95% CI = 24.2–

40.3) of cases, which is consistent with Houillie *et al.*, who found a 37% positivity rate by using the same cut-off value in defining high expression (cut-off 50%) (Houillier *et al.*, 2006).

In this study high p53 protein expression was found in all cases of secondary GBMs compared with only half of primary GBMs; in addition, the mean p53 labelling index was considerably higher in secondary GBMs (98.6 versus 32.7). This observation is also supported by other researches indicating a high rate of TP53 gene mutations and p53 protein overexpression in secondary GBMs (Ohgaki and Kleihues, 2007; Takano *et al.*, 2012; Watanabe *et al.*, 1996). Using a cut-off of 10%, in this study 75.0% (95% CI = 55.1–88.0) of DAs showed high p53 expression in close agreement with Gillet *et al.*, wherein, with a cut-off of 10%, 75% of DA cases also showed p53 overexpression (Gillet *et al.*, 2014).

In this study, there was no statistically significant difference in p53 protein expression between GBMs and DAs ($p = 0.416$) in relation to other studies with similar results (Ali and Jalal, 2013; Nayak *et al.*, 2004). In the current study, p53 protein expression had no prognostic significance either in GBMs ($p = 0.831$) or in DAs ($p = 0.330$), similarly to many studies that have failed to identify a prognostic role of p53 overexpression (Houillier *et al.*, 2006; Simmons *et al.*, 2001; Takano *et al.*, 2012).

In the current study, p53 expression had correlations with Ki-67 ($rs = 0.196$; $p = 0.027$), PDGFRA ($rs = 0.181$; $p = 0.043$) and MVD ($rs = 0.228$; $p = 0.031$) in GBMs. As regards p53 correlation with PDGFRA, both TP53 and PDGFRA gene mutations are more frequently associated with the proneural subtype of GBMs, as described by Verhaak *et al.* (Verhaak *et al.*, 2010).

p21

The p21 protein is an important cell cycle inhibitor that can bind to cyclin-dependent kinase (CDK) complexes and induce cell cycle arrest (Coqueret, 2003). A large number of studies been shown that p21 may have a dual role, and together with the tumour suppressor effect it may also act as an oncoprotein because of its antiapoptotic properties (De la Cueva *et al.*, 2006; Gartel, 2006). In the current study, high p21 expression was found in 49.3% (95% CI = 41.3–57.4) of GBMs, compared with 15% (95% CI = 5.2–36.0) of DAs, which is consistent with data in other studies that have found higher p21 positivity rates in high-grade gliomas (Zolota *et al.*, 2008). Paradoxically, high-grade gliomas – the more malignant and proliferative tumours – had higher p21 expression than low-grade gliomas, which may indicate that p21 expression in gliomas may contribute to its oncoprotein function. In this study, decreased p21 expression was statistically significantly more frequent in GBMs of a larger size (exceeding 4 cm) ($z = -2.460$; $p = 0.014$). This association was also supported by a negative correlation between p21 and the largest diameter of the tumour ($rs = -0.181$; $p = 0.045$). These results suggest that decreased p21 expression is involved in processes controlling tumour growth in line with the function of p21 as a tumour suppressor protein that is capable of cell cycle inhibition (Abbas and Dutta, 2009; Warfel and El-Deiry, 2013).

In DAs, in this study, a positive correlation between p21 and MVD was found ($r_s = 0.448$; $p = 0.049$), suggesting the possible role of p21 in angiogenesis. There is some evidence in the literature that p21, besides its antiapoptotic effect, can enhance tumour growth by promoting angiogenesis in cancer cells (Kuljaca *et al.*, 2009; Lee *et al.*, 2010).

p27

p27 is another cell cycle inhibitor that belongs to the same CIP/Kip family of CDK inhibitors as the p21 protein (Moller, 2000). Recent evidence suggests this dysregulation and reduced levels of p27 in human cancers may be attributed to post-translation mechanisms, especially the removal of p27 by degradating it in the ubiquitine-proteosome pathway (Bloom and Pagano, 2003; Piva *et al.*, 1999). In this study, high expression of p27 (with a cut-off of 70%) was noted in 60.1% (95% CI = 50.9–68.7) of GBMs. The data from this study were very similar to the results reported by Yang *et al*; this team found high expression of p27 (with a cut-off of 70%) in 57.2% of high-grade gliomas (Yang *et al.*, 2011). In this study, p27 expression in DAs was found in 86.9% of cases (95% CI = 67.8–95.4), in contrast to 92.8% and 81.2% in other studies with the same cut-off values (Faria *et al.*, 2007; Yang *et al.*, 2011). In this study, the mean amount of positive cells was significantly higher in DAs than in GBMs – 86.6% (95% CI = 81.6–91.7) versus 69.7% (95% CI = 65.8–73.7) – indicating that loss of p27 expression is associated with increased malignancy. Most studies supported decreased p27 expression rates in high-grade compared to low-grade gliomas (Faria *et al.*, 2007; Kirla *et al.*, 2003; Yang *et al.*, 2011; Zolota *et al.*, 2008). However, a trend towards a negative correlation between p27 and Ki-67 was found in this study in GBMs ($r_s = -0.199$; $p = 0.055$), indicating that loss of p27 is associated with a more aggressive and proliferative phenotype in GBMs. An inverse correlation between Ki-67 and p27 in gliomas was also supported by other authors (Cavalla *et al.*, 1999; Fuse *et al.*, 2000; Kirla *et al.*, 2003). Surprisingly, in this study an association between nuclear p27 levels and gender was found. Thus, p27 protein expression was statistically significantly lower in females ($z = -2.174$; $p = 0.030$). This finding does not contradict results that had been shown by Huang *et al*: this team of researchers found that oestrogens promote but progesterone inhibits nuclear p27 destruction by regulating

ubiquitin-proteasome system activity in endometrial cancer cells (Huang *et al.*, 2012). To the best of our knowledge, gender differences in p27 expression have not been described in gliomas. But we suppose that sex hormones may be implicated in the biological diversity of gliomas and can modify the molecular profile of glioma cells. In addition to this finding, an association between Ki-67 and gender has been discussed before.

CD44

CD44 is a transmembrane glycoprotein that serves as a major surface hyaluronic acid receptor and is involved in cell matrix adhesion, cell migration and various cellular signalling pathways (Dzwonek and Wilczynski, 2015; Naor *et al.*, 1997). Its membranous localization may be important in facilitating the invasion of neoplastic cells via CD44-hyaluronan interaction (Bradshaw *et al.*, 2016). CD44 engagement with hyaluronan is also suggested to enhance tumour progression through increased tyrosine kinase activity and resistance to treatment, accentuating this molecular association as a desirable treatment target (Mooney *et al.*, 2016; Shepard, 2015; Thapa and Wilson, 2016). CD44 has multiple isoforms due to splicing and post-translational modification and is characterized by high functional diversity (Prochazka *et al.*, 2014). CD44 was described as a cancer stem cell marker in different tumours, including glioblastoma. In the nervous system, CD44 has been identified as a marker of neural stem cells as well as astrocyte and oligodendrocyte precursors (Liu *et al.*, 2004; Naruse *et al.*, 2013). Some authors have also noted that in glioblastoma CD44 functions as a neural progenitor cell marker that is expressed on partially differentiated cells (Bradshaw *et al.*, 2016). CD44 is involved in mesenchymal transformation of tumour cells and enhances the invasiveness by promoting the adhesion (Xu *et al.*, 2015). In the molecular classification of glioblastoma, CD44 was described as a marker of mesenchymal subtype (Phillips *et al.*, 2006;

Verhaak *et al.*, 2010). It has been suggested that the immunohistochemical assessment of CD44 should become a mainstay in the molecular typing of glioblastomas as an economically effective surrogate method (Popova *et al.*, 2014). In this study, CD44 expression strongly depended on tumour grade, with the highest expression levels seen in GBMs. The mean expression value of CD44 in GBMs was 74.1% (95% CI = 69.6–78.7) versus 13.5% (95% CI = 7.7–19.2) in DAs. High CD44 expression (with a cut-off of 50%) was found in 81.5% (95% CI = 74.4–86.9) of GBMs, but no DAs had CD44 expression above this level. In comparison with this study, Popova *et al.* had found high CD44 expression in 42% of GBMs and 15% of DAs by using the same cut-off point (Popova *et al.*, 2014). However, Ranuncolo *et al.*, by using a higher cut-off point of 70%, had found high CD44 expression in 59% of GBMs and 9.5% of low-grade gliomas (Ranuncolo *et al.*, 2002). A few studies have specified the CD44 staining pattern in glioma tissues. The most prominent and typical is membranous, surface staining of CD44; this staining pattern was intense and was found in all GBMs in this study. However, such a membranous staining pattern was identified in a few DAs and it was patchy and vague. In contrast, all DAs had faint, barely noticeable CD44 immunoreactivity in cytoplasmic processes of astrocytes, creating a branched, delicate network of CD44 immunopositivity. In this study, weak, diffuse CD44 expression was not counted quantitatively and it did not account for assessment positive cases of DAs; however, it should be noted as a different staining pattern in low-grade gliomas. One study described a similar staining pattern in gliomas: membranous staining was found only in GBMs, but weak staining in processes of astrocytes characterized DAs (Jijiwa *et al.*, 2011). Interestingly, different authors described the occurrence of CD44 expression within processes of some fibrillary astrocytes in normal human brain (Kaaijk *et al.*, 1997; Sosunov *et al.*, 2014). Kaaijk *et al.* hypothesized that CD44 expression in normal astrocytes might contribute to the migratory capacity of

astrocytes upon inflammation and other injury (Kaaijk *et al.*, 1997). However, Lui *et al.* showed that CD44 expression identifies astrocyte-restricted precursor cells (Liu *et al.*, 2004). In many other recent studies, CD44 has also been identified as a marker of astrocyte precursor cells (Cai *et al.*, 2012; Malik *et al.*, 2014; Naruse *et al.*, 2013). Thus, we suppose that the weak background of CD44 immunoreactivity in processes may indicate on stemness and precursor state of neoplastic astrocytes in DAs. However, in high-grade gliomas, to achievem more aggressive behaviour and increased invasive properties of tumour cells, CD44 is significantly upregulated on the surface of neoplastic cells.

In this study, no prognostic role of CD44 was found in GBMs and DAs. However, CD44 was used as a mesenchymal marker in the subtyping of GBMs, and it was found that GBM, which belongs to the mesenchymal subtype (high CD44 expression and low p53, PDGFRA, IDH1 expression), had no response to radiotherapy. Thus, expression of CD44 can be used as a predictive marker in combination with other markers of proneural signature. Interestingly, in this study, in GBMs, CD44 expression was higher in females ($z = -2.224$; $p = 0.026$), indicating that the glioma stem cell population may be altered by gender-specific factors. In addition, CD44 showed a weak, statistically significant, negative correlation with GBM size ($rs = -0.314$; $p < 0.001$). This correlation was also confirmed by the association between the size and CD44 expression: higher CD44 expression values were more frequently found in GBMs of a smaller size (< 4 cm) than in larger-sized tumours (≥ 4 cm) ($z = -2.364$; $p = 0.018$), indicating that expansion and rapid growth of a tumour may lead to depletion of the stem cell population in glioma.

In DAs, CD44 expression had a negative correlation with PDGFRA ($r_s = -0.592$; $p = 0.006$). In addition, Conroy *et al.* showed that high CD44 scores were rarely found in gliomas with high PDGFRA expression (Conroy *et al.*, 2014). Cautiously considering that PDGFRA pathway activation in different

classifications has been considered as marker of proneural/proneural-like glioblastoma but CD44 expression points towards the mesenchymal subtype, a negative association seems to be more reasonable.

In DAs, CD44 expression also had a positive correlation with MVD (r_s = 0.490; p = 0.018); this may indicate that expansion of the stem cell population accelerates vascularization of tumour tissues, which enables an increased supply of blood and nutrients essential for tumour growth and progression. It was proved in several studies that glioma stem cells have a critical role in tumour angiogenesis and are capable of secreting several angiogenic substances (Bao *et al.*, 2006; Hardee and Zagzag, 2012).

PDGFRA

PDGFRA is a cell surface tyrosine kinase receptor for platelet-derived growth factor (PDGF). In the central nervous system, PDGFRA is the key molecule involved in the formation of mature oligodendrocytes. PDGFRA is expressed on oligodendrocyte precursor cells and even more multipotent neural stem cells, which give rise to mature oligodendrocytes if stimulated by PDGF-A (Fruttiger *et al.*, 1999; Hu *et al.*, 2008). PDGFRA signalling is also important in developing the neoplastic process, including gliomagenesis. Increased PDGF signalling in these immature, precursor cells stimulates their proliferation and blocks their ability to achieve a mature, differentiated cell state, causing them to form tumour-like growths resembling astrocytomas; continuing the proliferation of these precursor cells might lead to the development of astrocytomas (Jackson *et al.*, 2006).

According to Verhaak *et al.*, *PDGFRA* gene amplification together with mutations of *IDH1* and *TP53* characterize the proneural subtype of GBM (Verhaak *et al.*, 2010).

In this study, mean expression of PDGFRA was significantly higher in DAs – 42.3 (95% CI = 25.7–59.0) – than in GBMs – 7.9 (95% CI = 5.0–10.7). With a cut-off level of 50%, high PDGFRA expression was found in 50% (95% CI = 30.1–75.0) of DAs and only in 6.2% (95% CI = 3.2–11.3) of GBMs. The data is comparable with other studies: for example, Popova *et al.*, using the same cut-off value of 50%, reported strong PDGFRA positivity in 23% of DAs and 4% of GBMs (Popova *et al.*, 2014). In this study, PDGFRA expression correlates with p53 protein expression in both GBMs ($r_s = 0.181$; $p = 0.043$) and DAs ($r_s = 0.544$; $p = 0.013$). Correlation between p53 and PDGFRA expression in gliomas was also found by other researchers: for example, Popova *et al.* reported such a correlation in DAs and anaplastic astrocytomas but not in GBMs (Popova *et al.*, 2014). As mentioned before, both TP53 and PDGFRA gene mutations are frequently associated with the proneural subtype of GBMs, as shown by Verhaak *et al.* (Verhaak *et al.*, 2010). Correlation between p53 and PDGFRA may indicate some functional link – possibly defects in the TP53 gene and PDGFRA overexpression may increase the tumorigenic potential in a subset of gliomas – however, the possible mechanism explaining this correlation is not known.

In this study, another negative correlation between PDGFRA and CD44 ($r_s = -0.592$; $p = 0.006$) may explain this disagreement regarding PDGFRA and MVD. Returning to the negative correlation between PDGFRA and CD44 ($rs = -0.592$; $p = 0.006$), it indicates the existence of two mutually exclusive molecular signatures in gliomas, according to Verhaak *et al*. Surprisingly, PDGFRA expression also showed a negative correlation with MVD in DAs ($r_s = -0.501$; $p = 0.034$). Thus, upregulation of PDGFRA led to downregulation of CD44 – the potential glioma stem cell marker – however, the decreased population of stem cells suppressed angiogenesis, probably because of the deficiency of angiogenic factors produced by the same stem cells.

IDH1 R132H

Isocitrate dehydrogenase (IDH) is a metabolic enzyme with an important role in the citric acid cycle. Three isoforms of IDH are known, encoded by five related genes. IDH3 converts isocitrate to alpha-ketoglutarate and NAD+ to NADH in the Krebs cycle, and IDH1 catalyses oxidative decarboxylation of isocitrate to alpha-ketoglutarate and NADP+ to NADPH in the cytoplasm, and IDH2 in the mitochondria (Cohen *et al.*, 2013; Zhang *et al.*, 2013). IDH1 R132H, the most frequent mutation of the *IDH1* gene in glioma, results in the missense replacement of arginine by histidine, leading to production of the mutant enzyme that catalyses the synthesis of oncometabolite 2-hydroxyglutarate (Garber, 2010; Ward *et al.*, 2012). IDH1 mutations are early events in the development of gliomas, thus the majority of DAs and secondary GBMs bear this signature. Immunohistochemical detection of IDH1 R132H protein is a routine practice nowadays in distinguishing between primary and secondary GBMs that have a better prognosis. In the whole group of glioblastomas, secondary GBMs constitute 6–13 % of these tumours (Ohgaki and Kleihues, 2013). A significantly lower frequency (3.4%; 95% CI = 0.5–6.3) of secondary GBMs was observed in our study, probably due to the study design. In the present investigation, recurrent brain tumours were excluded as the previous therapy might be a confounding factor that could affect the molecular characteristics of gliomas (Parsons *et al.*, 2008; Safa *et al.*, 2015; Shankar *et al.*, 2014). A similar group was assessed by Nobusawa *et al*., who reported a very similar frequency of *IDH1* mutations: namely, 3.7% of cases clinically presenting as primary glioblastomas were identified as secondary GBMs by molecular signature (Nobusawa *et al.*, 2009).

In regard to DAs, expression of mutant IDH1 R132H protein was detected in 76.9% (95% CI = 60.7–93.1) of tumours, and the remaining 23.1% (6.9–39.3) were negative for IDH1 R132H mutation. The frequency of IDH1 mutations in low-grade gliomas is 80% and 87% (Christensen *et al.*, 2011; Juratli *et al.*, 2012);

however, the most frequent specific mutation – IDH1 R132H – was detected by immunohistochemistry in 57–80 % of low-grade gliomas (Cai *et al.*, 2016; Popova *et al.*, 2014; Wang *et al.*, 2016), which is also consistent with this study. The presence of IDH1 gene mutation is one of the known prognostic factors of more favourable prognosis in patients with high-grade gliomas (Gravendeel *et al.*, 2010; Nobusawa *et al.*, 2009; Parsons *et al.*, 2008; Sanson *et al.*, 2009). For example, the median overall survival rates of mutated and non-mutated IDH 1 patients with GBMs were 3.8 and 1.1 years (Parsons *et al.*, 2008). In this study, patients with secondary GBMs had a significantly better prognosis than those with primary GBMs – the median OS was 18.3 (95% CI = 18.0–18.5) months versus 7.7 (95% CI = 6.3–9.0) months ($p = 0.040$).

In this study, an association between IDH1 and p53 was also found in GBMs ($z = -3.555$; $p = 0.001$), as it was confirmed by other authors that these two abnormalities frequently coexist (Huang, 2019). In addition, both IDH1 and TP53 gene mutations characterize the proneural subtype of GBMs (Verhaak *et al.*, 2010).

MVD (by CD34)

Sustained angiogenesis is one of six essential hallmarks of neoplastic cells (Hanahan and Weinberg, 2000), and CD34, as an endothelial marker, is useful in studies of angiogenesis for determining microvascular density (MVD) and vascular patterns of neoplasms (Foote *et al.*, 2005; Weidner, 2008). The simple and easily reproducible quantitative method for determination of MVD in tumours was suggested by Weidner *et al.*, and Weidner's approach has been widely adopted in angiogenesis studies (Weidner *et al.*, 1991).

In this study, GBMs showed statistically significantly higher MVD values than DAs: the mean number of vessels per high-power field (hpf) (400x) was 40.7 (95% CI = 35.8–45.6) and 18.1 (95% CI = 12.9–23.3). This result is similar to

results reported by Zhang *et al*: 45 ± 6.2 vessels per hpf and 28 ± 7.2 vessels per hpf (Zhang *et al.*, 2014). In this study, no prognostic value of MVD was found in either GBMs or DAs. There were few studies on the prognostic role of MVD in brain tumours. Some studies indicated the prognostic significance of MVD in gliomas (Abdulrauf *et al.*, 1998; Leon *et al.*, 1996), however others rejected any prognostic role of MVD (Schiffer *et al.*, 1999). In one recent meta-analysis it was suggested that MVD could have prognostic significance in gliomas and more studies are essential in this regard (Fan *et al.*, 2019).

3.4. Molecular subtypes of gliomas

For a long time, two GBM subtypes were known, reflecting different pathogenetic pathways: primary GBMs, which develop *de novo,* and secondary GBMs, which result from progression from lower-grade glial neoplasm (Kleihues and Ohgaki, 1999). Both GBM subtypes are morphologically indistinguishable, and only clinical information about pre-existing low-grade glioma may help to differentiate between primary and secondary GBMs carrying different prognoses. Thus, morphologically GBM represented a single entity with almost the same prognostic significance. But the situation changed dramatically when The Cancer Genome Atlas (TCGA) project shed more light on the molecular basis of GBMs. So far, the TCGA project has produced a huge amount of data, including whole genomic sequence, expression and epigenetic analysis of many cancers, including GBMs. Verhaak *et al.*, using data generated by the TCGA project, found that GBMs can be divided into four molecular subtypes based on different molecular alterations and gene expression patterns: classical, mesenchymal, proneural and neural subtypes (Verhaak *et al.*, 2010). Because molecular techniques are complex, time-consuming and expensive they are not practical in routine. Immunohistochemistry (IHC) is an important component of pathology laboratory testing and a good surrogate of more

expensive traditional cytogenetic and molecular methods. Based on molecular signatures described by Verhaak *et al.*, several research teams have successfully applied IHC in molecular subtyping of gliomas (Conroy *et al.*, 2014; Le Mercier *et al.*, 2012; Motomura *et al.*, 2012; Popova *et al.*, 2014). In one study by Le Mercier *et al.*, classical-like and proneural-like subtypes of GBMs were recognized using IHC and a minimal amount of markers (p53, EGFR, PDGFRA), and the tumours that did not fit any expression pattern were classified as "Other" (Le Mercier *et al.*, 2012). In this study, a similar approach was used. Based on the study of Verhaak *et al.*, we chose to assess the expression of PDGFRA, IDH1 R132H, p53 and CD44 in order to classify GBM as a proneural or mesenchymal subtype. Our approach comes from the finding that mutations in TP53, IDH1 and PDGFRA genes are commonly associated with the proneural but not the mesenchymal subtype of GBM (Verhaak *et al.*, 2010).

In this study, 50% (95% CI = 42.0–58.0) of GBMs were classified as the proneural subtype, which is lower than in the study by Le Mercier *et al.*, where proneural-like subtype was present in 60.2% of cases defined by p53 and PDGFRA immunopositivity (Le Mercier *et al.*, 2012). Popova *et al.* reported the proneural subtype in 29% of GBMs using p53 and OLIG2 (Popova *et al.*, 2014). In this study, 18.5% (95% CI = 13.0–25.6) of GBMs were of the mesenchymal subtype. In other studies, the mesenchymal subtype was reported in 12% to 29% of GBM cases by using different mesenchymal markers such as CD44, MERTK, VIM and YKL40 (Conroy *et al.*, 2014; Popova *et al.*, 2014; Verhaak *et al.*, 2010). In the current study, no statistically significant associations were found between molecular subtype and clinical or remaining immunohistochemical parameters (MVD, Ki-67, p21 and p27) that were not used for subtyping. In the current study, no survival differences were found between different subtypes. With regard to clinical outcome, the mesenchymal subtype is described as a subtype with an unfavourable prognosis, in contrast to the proneural subtype, which is

characterized by better prognosis (Lin *et al.*, 2014; Phillips *et al.*, 2006; Verhaak *et al.*, 2010).

However, the response to adjuvant therapy differed between proneural and mesenchymal subtypes. In the current study, for GBM patients with a proneural subtype, there was a tendency for the addition of chemotherapy to radiotherapy alone to improve overall survival ($p = 0.061$) and for radiotherapy alone to significantly improve patients' overall survival compared with palliative management and surgery only without adjuvant treatment ($p = 0.008$). However, for GBM patients of the mesenchymal subtype, the addition of chemotherapy to radiotherapy alone significantly improved overall survival ($p = 0.002$), but radiotherapy alone showed no beneficial effect when compared with palliative management and surgery only without adjuvant treatment ($p = 0.857$), indicating radioresistancy of the mesenchymal subtype of GBM. Previously, Brown *et al.* reported the radioresistancy of the mesenchymal subtype while preserving the chemosensitivity of the mesenchymal subtype (Brown *et al.*, 2015). Several authors have reported that the mesenchymal subtype is associated with the stem cell phenotype, enriched with the presumed stem cell marker CD44 (Cheng *et al.*, 2012). However, glioma mesenchymal stem cells are characterized by extensive radioresistancy (Mao *et al.*, 2013; Nakano, 2015), which may explain the failure of the radiotherapeutic effect in the mesenchymal subtype of GBMs in this study. A more aggressive course, radioresistancy and expression of CD44 on mesenchymal stem cells of GBM were also supported by Mao *et al.* using experimental mouse glioma models and stem cell cultures (Mao *et al.*, 2013). In terms of DAs, the significance of subtyping in low-grade gliomas should be further evaluated. The low-grade gliomas are enriched mainly with markers for the proneural subtype (Cooper *et al.*, 2010; Guan *et al.*, 2014) . In addition, the high frequency of IDH1 mutations in low-grade gliomas constitutes the predominance of the proneural subtype (Kim *et al.*, 2010). In this study, most DAs belong to the proneural subtype – 24/26 (92.3%; 95% CI = 75.8–97.9) – while the remaining 2/26 (7.6%; 95% CI = 2.1% – 24.1%) DAs were not

otherwise classified. Because CD44 expression was very low in DAs with a median value of 8.5% (IQR = 15) and the mesenchymal subtype was not identified in DAs, mesenchymal signature might be of importance only in GBMs, and not in DAs.

Conclusions

1. The median survival of the studied patients with GBM is 7.9 months, which is slightly below the survival rates reported in other countries.
2. Patients with secondary GBMs (IDH-mutant) show significantly better prognosis than patients with primary GBMs (IDH-wild type), thus the presence of IDH1 R132H mutation is the most significant prognostic factor of better survival.
3. In patients with DAs, high PDGFRA expression is associated with significantly better survival.
4. CD44, p21, p27, PDGFRA and proliferation rate (by Ki-67) are grade-specific parameters in gliomas, thus CD44, Ki-67 and p21 are significantly upregulated; however, p27 and PDGFRA are downregulated in GBM. In contrast, p53 expression is grade independent in gliomas.
5. The immunohistochemical profile of gliomas involving expression of p27 and CD44 in GBMs and cellular proliferation (Ki-67) in both GBMs and DAs can be determined by gender-specific factors.
6. In GBMs, decreased expression of both p21 and CD44 is associated with larger tumours. In contrast, multifocal GBMs more frequently have a loss of p27 and higher expression of PDGFRA.
7. In gliomas, cell cycle proteins, such as p53, p21 and p27, are involved in molecular mechanisms that regulate proliferation and angiogenesis as reflected by Ki-67 and MVD, respectively.
8. PDGFRA expression correlates with p53 expression in both GBMs and DAs, indicating a strong functional link between these proteins. In DAs, PDGFRA correlates inversely with CD44, p21 and MVD.
9. Immunohistochemical subtyping of gliomas is possible by using a limited number of markers – PDGFRA, p53, IDH1 R132H and CD44. Expression

of CD44 is a reliable indicator of mesenchymal subtype in GBM, which has a worse response to radiotherapy.

Practical recommendations

1. Immunohistochemical visualization is recommended for all surgically resected glioma material for prognostic and predictive reasons.
2. Detection of IDH1 R132H mutation by IHC is recommended for all GBMs where it allows secondary GBMs to be distinguished from primary GBMs and thus IDH1 R132H is a valuable prognostic marker. The staining protocol developed during the study is recommended for routine use.
3. Detection of IDH1 R132H mutation by IHC is also recommended for DAs as an important and sensitive diagnostic test. Because the majority of DAs are IDH1 mutant tumours, IDH1 R132H immunohistochemistry could be helpful for precisely diagnosing infiltrating low-grade glioma, especially in small, limited tissue material such as stereotactic biopsies.
4. Detection of PDGFRA expression by IHC is recommended for DA, taking into account the significant association with survival.
5. Immunohistochemical classification of gliomas is possible and applicable in routine practice by using IHC; for the prediction of treatment response assessment of CD44 it is recommended to distinguish the mesenchymal subtype of GBM with more pronounced radioresistancy.

References

1. Abbas, T. and Dutta, A. (2009). p21 in cancer: intricate networks and multiple activities. *Nat Rev Cancer,* 9, 400–414.
2. Abdulrauf, S. I., Edvardsen, K., Ho, K. L., et al. (1998). Vascular endothelial growth factor expression and vascular density as prognostic markers of survival in patients with low-grade astrocytoma. *J Neurosurg,* 88, 513−520.
3. Ahmadloo, N., Kani, A. A., Mohammadianpanah, M., et al. (2013). Treatment outcome and prognostic factors of adult glioblastoma multiforme. *J Egypt Natl Canc Inst,* 25, 21–30.
4. Ali, T. and Jalal, J. (2013). Immunohistochemical expression of p53 and p21 in gliomas: a clinicopathological study. *Zanco Journal of Medical Sciences,* 17, 435–442.
5. Arshad, H., Ahmad, Z. and Hasan, S. H. (2010). Gliomas: correlation of histologic grade, Ki67 and p53 expression with patient survival. *Asian Pac J Cancer Prev,* 11, 1637–1640.
6. Ashcroft, M. and Vousden, K. H. (1999). Regulation of p53 stability. *Oncogene,* 18, 7637−7643.
7. Back, M. F., Ang, E. L., Ng, W. H., et al. (2007). Improved median survival for glioblastoma multiforme following introduction of adjuvant temozolomide chemotherapy. *Ann Acad Med Singapore,* 36, 338–342.
8. Bao, S., Wu, Q., Sathornsumetee, S., et al. (2006). Stem cell-like glioma cells promote tumor angiogenesis through vascular endothelial growth factor. *Cancer Res,* 66, 7843–7848.
9. Bardin, A., Boulle, N., Lazennec, G., et al. (2004). Loss of ERbeta expression as a common step in estrogen-dependent tumor progression. *Endocr Relat Cancer,* 11, 537–551.
10. Barnard, R. O. and Geddes, J. F. (1987). The incidence of multifocal cerebral gliomas. A histologic study of large hemisphere sections. *Cancer,* 60, 1519–1531.
11. Bhat, K. P., Balasubramaniyan, V., Vaillant, B., et al. (2013). Mesenchymal differentiation mediated by NF-kappaB promotes radiation resistance in glioblastoma. *Cancer Cell,* 24, 331–346.
12. Bloom, J. and Pagano, M. (2003). Deregulated degradation of the cdk inhibitor p27 and malignant transformation. *Semin Cancer Biol,* 13, 41–47.
13. Bradshaw, A., Wickremsekera, A., Tan, S. T., et al. (2016). Cancer stem cell hierarchy in glioblastoma multiforme. *Front Surg,* 3, 21.
14. Brennan, C., Momota, H., Hambardzumyan, D., et al. (2009). Glioblastoma subclasses can be defined by activity among signal transduction pathways and associated genomic alterations. *PLoS One,* 4, e7752.
15. Brennan, C. W., Verhaak, R. G. W., McKenna, A., et al. (2013). The somatic genomic landscape of glioblastoma. *Cell,* 155, 462–477.

16. Buckner, J. C. (2003). Factors influencing survival in high-grade gliomas. *Semin Oncol,* 30, 10–14.
17. Burns, K. A. and Korach, K. S. (2012). Estrogen receptors and human disease: an update. *Arch Toxicol,* 86, 1491–1504.
18. Cai, J., Zhu, P., Zhang, C., et al. (2016). Detection of ATRX and IDH1-R132H immunohistochemistry in the progression of 211 paired gliomas. *Oncotarget,* 7, 16384–16395.
19. Cai, N., Kurachi, M., Shibasaki, K., et al. (2012). CD44-positive cells are candidates for astrocyte precursor cells in developing mouse cerebellum. *Cerebellum,* 11, 181–193.
20. Cancer Genome Atlas Research, N. (2008). Comprehensive genomic characterization defines human glioblastoma genes and core pathways. *Nature,* 455, 1061–1068.
21. Capelle, L., Fontaine, D., Mandonnet, E., et al. (2013). Spontaneous and therapeutic prognostic factors in adult hemispheric World Health Organization Grade II gliomas: a series of 1097 cases: clinical article. *J Neurosurg,* 118, 1157–1168.
22. Castelli, J., Feuvret, L., Haoming, Q. C., et al. (2016). Prognostic and therapeutic factors of gliosarcoma from a multi-institutional series. *J Neurooncol,* 129, 85–92.
23. Cavalla, P., Piva, R., Bortolotto, S., et al. (1999). p27/kip1 expression in oligodendrogliomas and its possible prognostic role. *Acta Neuropathol,* 98, 629–634.
24. Christensen, B. C., Smith, A. A., Zheng, S., et al. (2011). DNA methylation, isocitrate dehydrogenase mutation, and survival in glioma. *J Natl Cancer Inst,* 103, 143–153.
25. Cohen, A. L., Holmen, S. L. and Colman, H. (2013). IDH1 and IDH2 mutations in gliomas. *Curr Neurol Neurosci Rep,* 13, 345.
26. Conroy, S., Kruyt, F. A., Joseph, J. V., et al. (2014). Subclassification of newly diagnosed glioblastomas through an immunohistochemical approach. *PLoS One,* 9, e115687.
27. Coqueret, O. (2003). New roles for p21 and p27 cell-cycle inhibitors: a function for each cell compartment? *Trends Cell Biol,* 13, 65–70.
28. De la Cueva, E., Garcia-Cao, I., Herranz, M., et al. (2006). Tumorigenic activity of p21Waf1//Cip1 in thymic lymphoma. *Oncogene,* 25, 4128–4132.
29. Djalilian, H. R., Shah, M. V. and Hall, W. A. (1999). Radiographic incidence of multicentric malignant gliomas. *Surg Neurol,* 51, 554-557; discussion 557–558.
30. Dobes, M., Shadbolt, B., Khurana, V. G., et al. (2011). A multicenter study of primary brain tumor incidence in Australia (2000–2008). *Neuro Oncol,* 13, 783–790.
31. Dong, Q., Li, Q., Wang, M., et al. (2019). Elevated CD44 expression predicts poor prognosis in patients with low-grade glioma. *Oncol Lett,* 18, 3698–3704.
32. Duffau, H. and Capelle, L. (2004). Preferential brain locations of low-grade gliomas. *Cancer,* 100, 2622–2626.
33. Dzwonek, J. and Wilczynski, G. M. (2015). CD44: molecular interactions, signaling and functions in the nervous system. *Front Cell Neurosci,* 9, 175.

34. Fan, C., Zhang, J., Liu, Z., et al. (2019). Prognostic role of microvessel density in patients with glioma. *Medicine,* 98, e14695-e14695.
35. Faria, M. H., Patrocinio, R. M., Moraes Filho, M. O., et al. (2007). Immunoexpression of tumor suppressor genes p53, p21 WAF1/CIP1 and p27 KIP1 in humam astrocystic tumors. *Arq Neuropsiquiatr,* 65, 1114–1122.
36. Foote, R. L., Weidner, N., Harris, J., et al. (2005). Evaluation of tumor angiogenesis measured with microvessel density (MVD) as a prognostic indicator in nasopharyngeal carcinoma: results of RTOG 9505. *International Journal of Radiation Oncology*Biology*Physics,* 61, 745–753.
37. Fruttiger, M., Karlsson, L., Hall, A. C., et al. (1999). Defective oligodendrocyte development and severe hypomyelination in PDGF-A knockout mice. *Development,* 126, 457–467.
38. Fuse, T., Tanikawa, M., Nakanishi, M., et al. (2000). p27Kip1 expression by contact inhibition as a prognostic index of human glioma. *J Neurochem,* 74, 1393–1399.
39. Garber, K. (2010). Oncometabolite? IDH1 discoveries raise possibility of new metabolism targets in brain cancers and leukemia. *J Natl Cancer Inst,* 102, 926–928.
40. Gartel, A. L. (2006). Is p21 an oncogene? *Mol Cancer Ther,* 5, 1385–1386.
41. Giannopoulos, S. and Kyritsis, A. P. (2010). Diagnosis and management of multifocal gliomas. *Oncology,* 79, 306–312.
42. Gillet, E., Alentorn, A., Doukoure, B., et al. (2014). TP53 and p53 statuses and their clinical impact in diffuse low grade gliomas. *J Neurooncol,* 118, 131–139.
43. Gravendeel, L. A., Kloosterhof, N. K., Bralten, L. B., et al. (2010). Segregation of non-p.R132H mutations in IDH1 in distinct molecular subtypes of glioma. *Hum Mutat,* 31, E1186–1199.
44. Hanahan, D. and Weinberg, R. A. (2000). The hallmarks of cancer. *Cell,* 100, 57–70.
45. Hardee, M. E. and Zagzag, D. (2012). Mechanisms of glioma-associated neovascularization. *Am J Pathol,* 181, 1126–1141.
46. Hartman, J., Edvardsson, K., Lindberg, K., et al. (2009). Tumor repressive functions of estrogen receptor beta in SW480 colon cancer cells. *Cancer Res,* 69, 6100–6106.
47. Hegi, M. E., Diserens, A. C., Gorlia, T., et al. (2005). MGMT gene silencing and benefit from temozolomide in glioblastoma. *N Engl J Med,* 352, 997–1003.
48. Hermansen, S. K., Christensen, K. G., Jensen, S. S., et al. (2011). Inconsistent immunohistochemical expression patterns of four different CD133 antibody clones in glioblastoma. *Journal of Histochemistry and Cytochemistry,* 59, 391–407.
49. Ho, D. M., Hsu, C. Y., Ting, L. T., et al. (2003). MIB-1 and DNA topoisomerase II alpha could be helpful for predicting long-term survival of patients with glioblastoma. *Am J Clin Pathol,* 119, 715–722.
50. Houillier, C., Lejeune, J., Benouaich-Amiel, A., et al. (2006). Prognostic impact of molecular markers in a series of 220 primary glioblastomas. *Cancer,* 106, 2218–2223.

51. Hu, J. G., Fu, S. L., Wang, Y. X., et al. (2008). Platelet-derived growth factor-AA mediates oligodendrocyte lineage differentiation through activation of extracellular signal-regulated kinase signaling pathway. *Neuroscience,* 151, 138–147.
52. Huang, K.-T., Pavlides, S. C., Lecanda, J., et al. (2012). Estrogen and progesterone regulate p27kip1 levels via the ubiquitin-proteasome system: pathogenic and therapeutic implications for endometrial Cancer. *PLoS One,* 7, e46072.
53. Huang, L. E. (2019). Friend or foe-IDH1 mutations in glioma 10 years on. *Carcinogenesis,* 40, 1299–1307.
54. Jackson, E. L., Garcia-Verdugo, J. M., Gil-Perotin, S., et al. (2006). PDGFR alpha-positive B cells are neural stem cells in the adult SVZ that form glioma-like growths in response to increased PDGF signaling. *Neuron,* 51, 187–199.
55. Jijiwa, M., Demir, H., Gupta, S., et al. (2011). CD44v6 regulates growth of brain tumor stem cells partially through the AKT-mediated pathway. *PLoS One,* 6, e24217.
56. Jin, Q., Zhang, W., Qiu, X. G., et al. (2011). Gene expression profiling reveals Ki-67 associated proliferation signature in human glioblastoma. *Chin Med J (Engl),* 124, 2584–2588.
57. Johannessen, A. L. and Torp, S. H. (2006). The clinical value of Ki-67/MIB-1 labeling index in human astrocytomas. *Pathol Oncol Res,* 12, 143–147.
58. Johansen, M. L., Stetson, L. C., Vadmal, V., et al. (2020). Gliomas display distinct sex-based differential methylation patterns based on molecular subtype. *Neuro-Oncology Advances,* 2.
59. Johnson, D. R. and O'Neill, B. P. (2012). Glioblastoma survival in the United States before and during the temozolomide era. *J Neurooncol,* 107, 359–364.
60. Juratli, T. A., Engellandt, K., Lautenschlaeger, T., et al. (2013). Is there pseudoprogression in secondary glioblastomas? *Int J Radiat Oncol Biol Phys,* 87, 1094–1099.
61. Juratli, T. A., Kirsch, M., Robel, K., et al. (2012). IDH mutations as an early and consistent marker in low-grade astrocytomas WHO grade II and their consecutive secondary high-grade gliomas. *J Neurooncol,* 108, 403–410.
62. Kaaijk, P., Pals, S. T., Morsink, F., et al. (1997). Differential expression of CD44 splice variants in the normal human central nervous system. *J Neuroimmunol,* 73, 70–76.
63. Kaminska, B., Czapski, B., Guzik, R., et al. (2019). Consequences of IDH1/2 mutations in gliomas and an assessment of inhibitors targeting mutated IDH proteins. *Molecules (Basel, Switzerland),* 24, 968.
64. Kashi, A. S., Rakhsha, A. and Houshyari, M. (2015). Overall survival in adult patients with low-grade, supratentorial glioma: ten years' follow-up at a single institution. *Electron Physician,* 7, 1114–1120.
65. Kawasoe, T., Takeshima, H., Yamashita, S., et al. (2015). Detection of p53 mutations in proliferating vascular cells in glioblastoma multiforme. *J Neurosurg,* 122, 317–323.

66. Kfoury, N., Sun, T., Yu, K., et al. (2018). Cooperative p16 and p21 action protects female astrocytes from transformation. *Acta Neuropathologica Communications,* 6, 12.

67. Kim, W. and Liau, L. M. (2012). IDH mutations in human glioma. *Neurosurg Clin N Am,* 23, 471–480.

68. Kirla, R. M., Haapasalo, H. K., Kalimo, H., et al. (2003). Low expression of p27 indicates a poor prognosis in patients with high-grade astrocytomas. *Cancer,* 97, 644–648.

69. Kleinschmidt-DeMasters, B. K., Lillehei, K. O. and Varella-Garcia, M. (2005). Glioblastomas in the older old. *Arch Pathol Lab Med,* 129, 624–631.

70. Kozak, K. R. and Moody, J. S. (2009). Giant cell glioblastoma: a glioblastoma subtype with distinct epidemiology and superior prognosis. *Neuro Oncol,* 11, 833–841.

71. Kuljaca, S., Liu, T., Dwarte, T., et al. (2009). The cyclin-dependent kinase inhibitor, p21(WAF1), promotes angiogenesis by repressing gene transcription of thioredoxin-binding protein 2 in cancer cells. *Carcinogenesis,* 30, 1865–1871.

72. Kumar, N., Kumar, P., Angurana, S. L., et al. (2013). Evaluation of outcome and prognostic factors in patients of glioblastoma multiforme: a single institution experience. *Journal of Neurosciences in Rural Practice,* 4, S46-S55.

73. Kushnir, I. and Tzuk-Shina, T. (2011). Efficacy of treatment for glioblastoma multiforme in elderly patients (65+): a retrospective analysis. *Isr Med Assoc J,* 13, 290–294.

74. Larjavaara, S., Mäntylä, R., Salminen, T., et al. (2007). Incidence of gliomas by anatomic location. *Neuro Oncol,* 9, 319–325.

75. Le Mercier, M., Hastir, D., Moles Lopez, X., et al. (2012). A simplified approach for the molecular classification of glioblastomas. *PLoS One,* 7, e45475.

76. Lee, S., Bui Nguyen, T. M., Kovalenko, D., et al. (2010). Sprouty1 inhibits angiogenesis in association with up-regulation of p21 and p27. *Mol Cell Biochem,* 338, 255–261.

77. Leon, S. P., Folkerth, R. D. and Black, P. M. (1996). Microvessel density is a prognostic indicator for patients with astroglial brain tumors. *Cancer,* 77, 362-372.

78. Liang, Y., Diehn, M., Watson, N., et al. (2005). Gene expression profiling reveals molecularly and clinically distinct subtypes of glioblastoma multiforme. *Proc Natl Acad Sci U S A,* 102, 5814–5819.

79. Liu, Y., Han, S. S., Wu, Y., et al. (2004). CD44 expression identifies astrocyte-restricted precursor cells. *Dev Biol,* 276, 31–46.

80. Ma, X., Lv, Y., Liu, J., et al. (2009). Survival analysis of 205 patients with glioblastoma multiforme: clinical characteristics, treatment and prognosis in China. *J Clin Neurosci,* 16, 1595–1598.

81. Malik, N., Wang, X., Shah, S., et al. (2014). Comparison of the gene expression profiles of human fetal cortical astrocytes with pluripotent stem cell derived neural stem cells identifies human astrocyte markers and signaling pathways and transcription factors active in human astrocytes. *PLoS One,* 9, e96139.

82. Meis, J. M., Martz, K. L. and Nelson, J. S. (1991). Mixed glioblastoma multiforme and sarcoma. A clinicopathologic study of 26 radiation therapy oncology group cases. *Cancer,* 67, 2342–2349.

83. Moller, M. B. (2000). P27 in cell cycle control and cancer. *Leuk Lymphoma,* 39, 19–27.

84. Mooney, K. L., Choy, W., Sidhu, S., et al. (2016). The role of CD44 in glioblastoma multiforme. *J Clin Neurosci,* 34, 1–5.

85. Moskowitz, S. I., Jin, T. and Prayson, R. A. (2006). Role of MIB1 in predicting survival in patients with glioblastomas. *J Neurooncol,* 76, 193–200.

86. Motomura, K., Natsume, A., Watanabe, R., et al. (2012). Immunohistochemical analysis-based proteomic subclassification of newly diagnosed glioblastomas. *Cancer Sci,* 103, 1871–1879.

87. Naor, D., Sionov, R. V. and Ish-Shalom, D. (1997). CD44: structure, function, and association with the malignant process. *Adv Cancer Res,* 71, 241–319.

88. Naruse, M., Shibasaki, K., Yokoyama, S., et al. (2013). Dynamic changes of CD44 expression from progenitors to subpopulations of astrocytes and neurons in developing cerebellum. *PLoS One,* 8, e53109.

89. Nayak, A., Ralte, A. M., Sharma, M. C., et al. (2004). p53 protein alterations in adult astrocytic tumors and oligodendrogliomas. *Neurol India,* 52, 228–232.

90. Neder, L., Colli, B. O., Machado, H. R., et al. (2004). MIB-1 labeling index in astrocytic tumors--a clinicopathologic study. *Clin Neuropathol,* 23, 262–270.

91. Nobusawa, S., Watanabe, T., Kleihues, P., et al. (2009). IDH1 mutations as molecular signature and predictive factor of secondary glioblastomas. *Clin Cancer Res,* 15, 6002–6007.

92. Ohgaki, H. and Kleihues, P. (2007). Genetic pathways to primary and secondary glioblastoma. *Am J Pathol,* 170, 1445–1453.

93. Ohgaki, H. and Kleihues, P. (2013). The definition of primary and secondary glioblastoma. *Clin Cancer Res,* 19, 764–772.

94. Ortensi, B., Setti, M., Osti, D., et al. (2013). Cancer stem cell contribution to glioblastoma invasiveness. *Stem Cell Research & Therapy,* 4, 18.

95. Oszvald, A., Guresir, E., Setzer, M., et al. (2012). Glioblastoma therapy in the elderly and the importance of the extent of resection regardless of age. *J Neurosurg,* 116, 357–364.

96. Parsons, D. W., Jones, S., Zhang, X., et al. (2008). An integrated genomic analysis of human glioblastoma multiforme. *Science,* 321, 1807–1812.

97. Paruthiyil, S., Parmar, H., Kerekatte, V., et al. (2004). Estrogen receptor beta inhibits human breast cancer cell proliferation and tumor formation by causing a G2 cell cycle arrest. *Cancer Res,* 64, 423–428.

98. Paszat, L., Laperriere, N., Groome, P., et al. (2001). A population-based study of glioblastoma multiforme. *Int J Radiat Oncol Biol Phys,* 51, 100–107.

99. Phillips, H. S., Kharbanda, S., Chen, R., et al. (2006). Molecular subclasses of high-grade glioma predict prognosis, delineate a pattern of disease progression, and resemble stages in neurogenesis. *Cancer Cell,* 9, 157–173.

100. Piva, R., Cancelli, I., Cavalla, P., et al. (1999). Proteasome-dependent degradation of p27/kip1 in gliomas. *J Neuropathol Exp Neurol,* 58, 691–696.

101. Popova, S. N., Bergqvist, M., Dimberg, A., et al. (2014). Subtyping of gliomas of various WHO grades by the application of immunohistochemistry. *Histopathology,* 64, 365–379.

102. Prochazka, L., Tesarik, R. and Turanek, J. (2014). Regulation of alternative splicing of CD44 in cancer. *Cell Signal,* 26, 2234–2239.

103. Ranuncolo, S. M., Ladeda, V., Specterman, S., et al. (2002). CD44 expression in human gliomas. *J Surg Oncol,* 79, 30-35; discussion 35–36.

104. Raysi Dehcordi, S., De Paulis, D., Marzi, S., et al. (2012). Survival prognostic factors in patients with glioblastoma: our experience. *J Neurosurg Sci,* 56, 239–245.

105. Reis, R. M., Hara, A., Kleihues, P., et al. (2001). Genetic evidence of the neoplastic nature of gemistocytes in astrocytomas. *Acta Neuropathol,* 102, 422–425.

106. Roy, S., Lahiri, D., Maji, T., et al. (2015). Recurrent glioblastoma: where we stand. *South Asian J Cancer,* 4, 163–173.

107. Ryu, M. S., Park, H. J., Moon, C. M., et al. (2018). Expression of CD44 according to clinicopathologic characteristics of gastric cancer. *EMJ,* 41, 63–74.

108. Safa, A. R., Saadatzadeh, M. R., Cohen-Gadol, A. A., et al. (2015). Glioblastoma stem cells (GSCs) epigenetic plasticity and interconversion between differentiated non-GSCs and GSCs. *Genes Dis,* 2, 152–163.

109. Sanson, M., Marie, Y., Paris, S., et al. (2009). Isocitrate dehydrogenase 1 codon 132 mutation is an important prognostic biomarker in gliomas. *J Clin Oncol,* 27, 4150–4154.

110. Sareddy, G. R., Li, X., Liu, J., et al. (2016). Selective Estrogen Receptor beta Agonist LY500307 as a Novel Therapeutic Agent for Glioblastoma. *Sci Rep,* 6, 24185.

111. Schiffer, D., Bosone, I., Dutto, A., et al. (1999). The prognostic role of vessel productive changes and vessel density in oligodendroglioma. *J Neurooncol,* 44, 99–107.

112. Schomas, D. A., Laack, N. N., Rao, R. D., et al. (2009). Intracranial low-grade gliomas in adults: 30-year experience with long-term follow-up at Mayo Clinic. *Neuro Oncol,* 11, 437–445.

113. Schwartzbaum, J. A., Fisher, J. L., Aldape, K. D., et al. (2006). Epidemiology and molecular pathology of glioma. *Nat Clin Pract Neurol,* 2, 494-503; quiz 491 p following 516.

114. Scoccianti, S., Magrini, S. M., Ricardi, U., et al. (2010). Patterns of care and survival in a retrospective analysis of 1059 patients with glioblastoma multiforme treated between 2002 and 2007: a multicenter study by the Central Nervous System Study Group of Airo (italian Association of Radiation Oncology). *Neurosurgery,* 67, 446–458.

115. Scott, J. G., Bauchet, L., Fraum, T. J., et al. (2012). Recursive partitioning analysis of prognostic factors for glioblastoma patients aged 70 years or older. *Cancer,* 118, 5595–5600.

116. Shankar, A., Kumar, S., Iskander, A., et al. (2014). Subcurative radiation significantly increases cell proliferation, invasion, and migration of primary glioblastoma multiforme in vivo. *Chin J Cancer,* 33, 148–158.

117. Shepard, H. M. (2015). Breaching the castle walls: hyaluronan depletion as a therapeutic approach to cancer therapy. *Front Oncol,* 5, 192.

118. Shivaprasad, N. V., Satish, S., Ravishankar, S., et al. (2016). Ki-67 immunostaining in astrocytomas: association with histopathological grade – a South Indian study. *Journal of Neurosciences in Rural Practice,* 7, 510–514.

119. Simmons, M. L., Lamborn, K. R., Takahashi, M., et al. (2001). Analysis of complex relationships between age, p53, epidermal growth factor receptor, and survival in glioblastoma patients. *Cancer Res,* 61, 1122–1128.

120. Simpson, J. R., Horton, J., Scott, C., et al. (1993). Influence of location and extent of surgical resection on survival of patients with glioblastoma multiforme: results of three consecutive Radiation Therapy Oncology Group (RTOG) clinical trials. *Int J Radiat Oncol Biol Phys,* 26, 239–244.

121. Skjulsvik, A. J., Mørk, J. N., Torp, M. O., et al. (2014). Ki-67/MIB-1 immunostaining in a cohort of human gliomas. *International Journal of Clinical and Experimental Pathology,* 7, 8905–8910.

122. Sosunov, A. A., Wu, X., Tsankova, N. M., et al. (2014). Phenotypic heterogeneity and plasticity of isocortical and hippocampal astrocytes in the human brain. *The Journal of Neuroscience,* 34, 2285–2298.

123. Stupp, R., Brada, M., van den Bent, M. J., et al. (2014). High-grade glioma: ESMO Clinical Practice Guidelines for diagnosis, treatment and follow-up. *Ann Oncol,* 25 Suppl 3, iii93-101.

124. Stupp, R., Mason, W. P., van den Bent, M. J., et al. (2005). Radiotherapy plus concomitant and adjuvant temozolomide for glioblastoma. *N Engl J Med,* 352, 987–996.

125. Sun, T., Plutynski, A., Ward, S., et al. (2015). An integrative view on sex differences in brain tumors. *Cellular and Molecular Life Sciences,* 72, 3323–3342.

126. Takano, S., Kato, Y., Yamamoto, T., et al. (2012). Immunohistochemical detection of IDH1 mutation, p53, and internexin as prognostic factors of glial tumors. *J Neurooncol,* 108, 361–373.

127. Teo, W. Y., Sekar, K., Seshachalam, P., et al. (2019). Relevance of a TCGA-derived glioblastoma subtype gene-classifier among patient populations. 9, 7442.

128. Thapa, R. and Wilson, G. D. (2016). The importance of CD44 as a stem cell biomarker and therapeutic target in cancer. *Stem Cells Int,* 2016, 2087204.

129. Thota, B., Shukla, S. K., Srividya, M. R., et al. (2012). IDH1 mutations in diffusely infiltrating astrocytomas: grade specificity, association with protein expression, and clinical relevance. *Am J Clin Pathol,* 138, 177–184.

130. Thotakura, M., Tirumalasetti, N. and Krishna, R. (2014). Role of Ki-67 labeling index as an adjunct to the histopathological diagnosis and grading of astrocytomas. *J Cancer Res Ther,* 10, 641–645.

131. Tove, L.-L., Andreas Hanssøn, H., Stein, S., et al. (2012). Prognostic value of histological features in diffuse astrocytomas WHO grade II. *International Journal of Clinical and Experimental Pathology,* 5, 152–158.

132. Trabelsi, S., Chabchoub, I., Ksira, I., et al. (2016). Molecular diagnostic and prognostic subtyping of gliomas in Tunisian population. *Mol Neurobiol*.

133. Tugcu, B., Postalci, L. S., Gunaldi, O., et al. (2010). Efficacy of clinical prognostic factors on survival in patients with glioblastoma. *Turk Neurosurg,* 20, 117–125.

134. Ulutin, C., Fayda, M., Aksu, G., et al. (2006). Primary glioblastoma multiforme in younger patients: a single-institution experience. *Tumori,* 92, 407–411.

135. Valle-Folgueral, J. M., Mascarenhas, L., Costa, J. A., et al. (2008). Giant cell glioblastoma: review of the literature and illustrated case. *Neurocirugia (Astur),* 19, 343–349.

136. van Diest, P. J., van Dam, P., Henzen-Logmans, S. C., et al. (1997). A scoring system for immunohistochemical staining: consensus report of the task force for basic research of the EORTC-GCCG. European Organization for Research and Treatment of Cancer-Gynaecological Cancer Cooperative Group. *J Clin Pathol,* 50, 801–804.

137. Verger, E., Valduvieco, I., Caral, L., et al. (2011). Does gender matter in glioblastoma? *Clin Transl Oncol,* 13, 737–741.

138. Verhaak, R. G., Hoadley, K. A., Purdom, E., et al. (2010). Integrated genomic analysis identifies clinically relevant subtypes of glioblastoma characterized by abnormalities in PDGFRA, IDH1, EGFR, and NF1. *Cancer Cell,* 17, 98–110.

139. Wakimoto, H., Aoyagi, M., Nakayama, T., et al. (1996). Prognostic significance of Ki-67 labeling indices obtained using MIB-1 monoclonal antibody in patients with supratentorial astrocytomas. *Cancer,* 77, 373–380.

140. Wang, P.-f., Liu, N., Song, H.-w., et al. (2016). IDH-1(R132H) mutation status in diffuse glioma patients: implications for classification. *Oncotarget,* 7, 31393–31400.

141. Wang, X., Chen, J. X., Liu, J. P., et al. (2014). Gain of function of mutant TP53 in glioblastoma: prognosis and response to temozolomide. *Ann Surg Oncol,* 21, 1337–1344.

142. Ward, P. S., Cross, J. R., Lu, C., et al. (2012). Identification of additional IDH mutations associated with oncometabolite R(-)-2-hydroxyglutarate production. *Oncogene,* 31, 2491–2498.

143. Warfel, N. A. and El-Deiry, W. S. (2013). p21WAF1 and tumourigenesis: 20 years after. *Curr Opin Oncol,* 25, 52–58.

144. Watanabe, K., Tachibana, O., Sata, K., et al. (1996). Overexpression of the EGF receptor and p53 mutations are mutually exclusive in the evolution of primary and secondary glioblastomas. *Brain Pathol,* 6, 217-223; discussion 223–214.

145. Watanabe, K., Tachibana, O., Yonekawa, Y., et al. (1997). Role of gemistocytes in astrocytoma progression. *Lab Invest,* 76, 277–284.

146. Weidner, N. (2008). Chapter 14. Measuring intratumoral microvessel density. *Methods Enzymol,* 444, 305–323.

147. Weidner, N., Semple, J. P., Welch, W. R., et al. (1991). Tumor angiogenesis and metastasis: correlation in invasive breast carcinoma. *N Engl J Med,* 324, 1–8.

148. Xu, H., Tian, Y., Yuan, X., et al. (2015). The role of CD44 in epithelial–mesenchymal transition and cancer development. *OncoTargets and therapy,* 8, 3783–3792.

149. Yan, H., Parsons, D. W., Jin, G., et al. (2009). IDH1 and IDH2 mutations in gliomas. *N Engl J Med,* 360, 765–773.

150. Yang, J., Liao, D., Wang, Z., et al. (2011). Mammalian target of rapamycin signaling pathway contributes to glioma progression and patients' prognosis. *J Surg Res,* 168, 97–102.

151. Yang, P., Wang, Y., Peng, X., et al. (2013). Management and survival rates in patients with glioma in China (2004-2010): a retrospective study from a single-institution. *J Neurooncol,* 113, 259–266.

152. Yang, W., Warrington, N. M., Taylor, S. J., et al. (2019). Sex differences in GBM revealed by analysis of patient imaging, transcriptome, and survival data. *Science Translational Medicine,* 11, eaao5253.

153. Yu, C. P., Ho, J. Y., Huang, Y. T., et al. (2013). Estrogen inhibits renal cell carcinoma cell progression through estrogen receptor-beta activation. *PLoS One,* 8, e56667.

154. Zhang, C., Moore, L. M., Li, X., et al. (2013). IDH1/2 mutations target a key hallmark of cancer by deregulating cellular metabolism in glioma. *Neuro Oncol,* 15, 1114–1126.

155. Zhang, J., Yang, W. E. I., Zhao, D., et al. (2014). Correlation between TSP-1, TGF-β and PPAR-γ expression levels and glioma microvascular density. *Oncol Lett,* 7, 95–100.

156. Zolota, V., Tsamandas, A. C., Aroukatos, P., et al. (2008). Expression of cell cycle inhibitors p21, p27, p14 and p16 in gliomas. Correlation with classic prognostic factors and patients' outcome. *Neuropathology,* 28, 35–42.

Publications and reports on topics of the Doctoral Thesis

Publications

1. Molecular classification of diffuse gliomas. Jakovlevs, A., Vanags, A., Gardovskis, J., Strumfa, I. *Polish Journal of Pathology*. (2019). 70(4), 246–258. doi:10.5114/pjp.2019.93126. (Pubmed).
2. Biserova K, Jakovlevs A, Uljanovs R, Strumfa I. Cancer Stem Celis: Significance in Origin. Pathogenesis and Treatment of Glioblastoma. Cells. 2021; 10(3):62 l. (Pubmed)
3. Jakovļevs, A., Vanags, A., Gardovskis, J., & Štrumfa, I. (2020). Expression of CD44 and IDH1 R132H in Gliomas and their Prognostic Relevance, Proceedings of the Latvian Academy of Sciences. Section B. *Natural, Exact, and Applied Sciences.* 74(5).
4. Glioblastoma – Current Concepts, Prognostic Markers And Molecular Classification / Jakovlevs, A., Vanags, A., Balodis, D., Gardovskis, J., Strumfa, I. *Acta Chirurgica Latviensis*. - No. 13/1 (2013), p. 58–64.
5. Childhood medulloblastoma in Latvia: morphologic and molecular implications for diagnostics and personalised treatment / Franckevica, I., Jakovlevs, A., Abolins, A., Vanags, A., Strumfa, I., ...[et al.]. *Acta Chirurgica Latviensis*. - No. 16/1 (2016), p. 9–15.
6. Solitary and multiple meningiomas : an immunohistochemical comparison / Vikmane, B., Jakovlevs, A., Vanags, A., Strumfa, I. *Acta Chirurgica Latviensis.* - No. 15/1 (2015), p. 23–28.
7. Prolonged survival after neurosurgical resection of lung cancer metastasis / Jakovlevs, A., Vanags, A., Strumfa, I....[et al.]. *Acta Chirurgica Latviensis.* - No.14/1 (2014), p.32-34.

8. Recurrent multiple atypical meningiomas despite neurosurgical resection / Jakovlevs, A., Strumfa, I., Vanags, A. ...[et al.]. *Acta Chirurgica Latviensis*. - No. 14/2 (2014), p. 56–58.
9. Low-grade rhabdoid meningioma : unusual morphological characteristics / Jakovlevs, A., Vanags, A., Gardovskis, J., Strumfa, I. *Acta Chirurgica Latviensis.* - No.13/1 (2013), p. 84–86.

Reports and theses at international congresses and conferences

1. Jakovlevs, A., Gardovskis, J., Štrumfa, I. Ki-67 labeling index and CD44 expression in gliomas: does the gender matter? 10th Baltic Morphology Scientific Conference, 24.–25.10.2019, Kaunas, Lithuania. *Abstract Book*, page 262.
2. Jakovlevs, A., Gardovskis, J., Štrumfa, I. Prognostic impact and correlations of Ki-67 labeling index and CD44 expression in gliomas. 10th Baltic Morphology Scientific Conference, 24.–25.10.2019, Kaunas, Lithuania. *Abstract Book*, page 261
3. Dr. Arvids Jakovlevs, Prof. Ilze Strumfa, Prof. Janis Gardovskis. Prognostic Role of Ki-67 Labeling Index in Diffuse Gliomas. Rīga Stradiņš University International Conference on Medical and Health Care Sciences Knowledge; 01.04.-03.04. 2019, Riga, Latvia; *Abstract Book*, page 730.
4. Dr. Arvids Jakovlevs, Prof. Ilze Strumfa, Prof. Janis Gardovskis. Prognostic and Predictive Significance of Immunohistochemically Defined Molecular Subclasses in Glioblastoma. Rīga Stradiņš University International Conference on Medical and Health Care Sciences Knowledge, 01.–03.04. 2019, Riga, Latvia; *Abstract Book,* page 729.
5. Prof. Ilze Strumfa, Dr. Dz. Mezale, Prof. Guntis Bahs, Dr. med. Andrejs Vanags, Dr. Ilze Fridrihsone, Dr. A.Jakovlevs. Digital Pathology in

Education: Experience of Rīga Stradiņš University. Rīga Stradiņš University International Conference on Medical and Health Care Sciences Knowledge, 01.04.-03.04.2019, Riga, Latvia; *Abstract Book,* page 741.

6. Assessment of microvascular density in gliomas : diagnostic and prognostic significance. Jakovlevs, A., Vanags, A., Gardovskis, J., Strumfa, I. Baltic Morphology IX (Tartu, Estonia, Sept. 27–29, 2017): Conference Programme: Abstracts of Presentations / University of Tartu. - Tartu, 2017. - P. 34.
7. Pleomorphic xanthoastrocytoma – a rare type of cerebral glioma. Jakovlevs, A., Vanags, A., Gardovskis, J., Strumfa, I. Baltic Morphology IX (Tartu, Estonia, Sept. 27–29, 2017): Conference Programme : Abstracts of Presentations / University of Tartu. - Tartu, 2017. - P. 35.
8. Prognostic and predictive role of proneural and mesenchymal molecular signatures in glioblastoma. Jakovlevs, A., Vanags, A., Gardovskis, J., Strumfa, I. 8th Mildred Scheel Cancer Conference (Bonn, Germany, June 14–16, 2017): Programme and Abstracts. - Bonn, 2017. - P. 148.
9. Expression of aberrant p53 protein in medulloblastoma [Elektroniskais resurss]. Kirsakmens, G., Franckevica, I., Kolomencikova, L., Jakovlevs, A., Balodis, D., Strumfa, I. International Symposium "Targets of immunotherapy of chronic viral infections and cancer" (Riga, Latvia, May 24-26, 2016)[Elektroniskais resurss] : *Abstract Book*. - Riga, 2016. - 1 p., on CD.
10. p53 protein as a potential target of cancer vaccines in glioblastomas [Elektroniskais resurss]. Jakovlevs, A., Vanags, A., Gardovskis, J., Strumfa, I. International Symposium "Targets of immunotherapy of chronic viral infections and cancer" (Riga, Latvia, May 24–26, 2016) [Elektroniskais resurss] : *Abstract Book*. - Riga, 2016. - 1 p., on CD.

11. Jakovļevs, A. IDH1-R132 immunohistochemistry in human gliomas : a way to improved diagnostics. Jakovlevs, A., Vanags, A., Strumfa, I. Eesti Arst. - Suppl.2 (2015, Sept.), p.68. - 8th Congress of the Baltic Association of Surgeons (Tallinn, Estonia, Sept.10–12, 2015) : [Abstracts].
12. Jakovļevs, A. Immunohistochemical analysis of platelet-derived growth factor receptor-alpha (PDGFRA) expression in gliomas. Jakovlevs, A., Vanags, A., Strumfa, I. The 8th Baltic Morphology Scientific Conference "Interdisciplinary nature of contemporary morphology" (Vilnius, Lithuania, Nov. 12–14, 2015) : [Abstract Book] / Vilnius University. - Vilnius, 2015. - P. 90.
13. Jakovļevs, A. The spectrum of brain metastases. Jakovlevs, A., Vanags, A., Strumfa, I. The 8th Baltic Morphology Scientific Conference "Interdisciplinary nature of contemporary morphology" (Vilnius, Lithuania, Nov. 12–14, 2015) : [Abstract Book] / Vilnius University. - Vilnius, 2015. - P. 91.
14. Heterogeneity of Ki-67 and p53 expression in glioblastomas : [abstract]. Jakovlevs, A., Strumfa, I., Vanags, A., Gardovskis, J. Virchows Archiv. - Vol. 465, Suppl.1 (2014, Aug.), p. S352. - Starptautiski citējamā izdevumā. London. United Kingdom.
15. Lipoastrocytoma of the spinal cord mimicking lipoma : [abstract]. Jakovlevs, A., Strumfa, I., Vanags, A., Gardovskis, J. Virchows Archiv. - Vol.465, Suppl.1 (2014, Aug.), p.S353. - Starptautiski citējamā izdevumā. London. United Kingdom.

16. Low-grade rhabdoid meningioma - unusual morphological characteristics. Jakovļevs, A., Feldmane, L., Štrumfa, I., Gardovskis, J. Baltic Morphology VII Scientific Conference "Morphological sciences in the experimental and clinical medicine" (Rīga, Latvia, Nov. 7–9, 2013) : *Abstract Book* / Riga Stradiņš University. - Riga, 2013. - P. 85.

Reports and theses at Latvian (local) congresses and conferences

1. Prognostic role of CD44 expression in diffuse gliomas. Jakovļevs, A., Vanags, A., Gardovskis, J., Štrumfa, I. 2018. gada Zinātniskās konferences tēzes (Rīga, 2018.g. 22.–23.martā). Rīgas Stradiņa universitāte. - Rīga, 2018. - 165. lpp.
2. Survival analysis of patients with diffuse gliomas in Latvia. Jakovļevs, A., Vanags, A., Gardovskis, J., Štrumfa, I. 2018. gada Zinātniskās konferences tēzes (Rīga, 2018.g. 22.–23.martā). Rīgas Stradiņa universitāte. - Rīga, 2018. - 164. lpp.
3. p27 and p21 protein expression in gliomas and their prognostic relevance. Jakovlevs, A., Vanags, A., Gardovskis, J., Strumfa, I. 2017. gada Zinātniskās konferences tēzes (Rīga, 2017.g. 6.–7.aprīlī). Rīgas Stradiņa universitāte. - Rīga, 2017. - 210. lpp.
4. Prognostic role of platelet derived growth factor receptor alpha expression in diffuse gliomas. Jakovlevs, A., Vanags, A., Gardovskis, J., Strumfa, I. 2017. gada Zinātniskās konferences tēzes (Rīga, 2017.g. 6.–7.aprīlī). Rīgas Stradiņa universitāte. - Rīga, 2017. - 209. lpp.

5. IDH1 R132H mutanta proteīna ekspresijas biežums difūzās astrocitomās. Jakovļevs, A., Vanags, A., Gardovskis, J., Štrumfa, I. 2016. gada Zinātniskās konferences tēzes (Rīga, 2016.g. 17.–18.martā). Rīgas Stradiņa universitāte. - Rīga, 2016. - 191. lpp.
6. p21 un p53 proteīna ekspresija gliālos audzējos. Jakovļevs, A., Vanags, A., Štrumfa, I., Gardovskis, J. 2016. gada Zinātniskās konferences tēzes (Rīga, 2016. g. 17.–18.martā). Rīgas Stradiņa universitāte. - Rīga, 2016. - 192. lpp.
7. CD44 proteīna ekspresija gliālos audzējos. Jakovļevs, A., Vanags, A., Gardovskis, J., Štrumfa, I. 2015.gada Zinātniskās konferences tēzes (Rīga, 2015. g. 26.–27.martā). Rīgas Stradiņa universitāte. - Rīga, 2015. - 281. lpp.
8. Primārās un sekundārās glioblastomas operāciju materiālā pacientiem Latvijā. Jakovļevs, A., Vanags, A., Gardovskis, J., Āboliņš, A., Štrumfa, I. 2015. gada Zinātniskās konferences tēzes (Rīga, 2015. g. 26.–27.martā). Rīgas Stradiņa universitāte. - Rīga, 2015. - 280. lpp.
9. Anaplastiska hemangiopericitoma – rets smadzeņu apvalku audzējs. Jakovļevs, A., Vanags, A., Gardovskis, J., Štrumfa, I. ...[u. c.]. 2014. gada Zinātniskās konferences tēzes (Rīga, 2014. g. 10.–11. aprīlī). Rīgas Stradiņa universitāte. - Rīga, 2014. - 294. lpp.
10. Gliosarkoma – rets gliāls audzējs bērnu vecumā. Jakovļevs, A., Vanags, A., Gardovskis, J., Štrumfa, I. 2014. gada Zinātniskās konferences tēzes (Rīga, 2014. g. 10.–11. aprīlī). Rīgas Stradiņa universitāte. - Rīga, 2014. - 308. lpp.
11. Gliosarkomu diagnostiskie un prognostiskie marķieri. Jakovļevs, A., Vanags, A., Gardovskis, J., Štrumfa, I. 2014.gada Zinātniskās konferences tēzes (Rīga, 2014. g. 10.–11. aprīlī). Rīgas Stradiņa universitāte. Rīga, 2014. - 293. lpp.
12. Ki-67 proliferācijas indeksa un p53 proteīna ekspresijas heterogenitāte glioblastomās. Jakovļevs, A., Vanags, A., Gardovskis, J., Štrumfa, I. 2014.

gada Zinātniskās konferences tēzes (Rīga, 2014. g. 10.–11. aprīlī). Rīgas Stradiņa universitāte. - Rīga, 2014. - 309. lpp.

13. CNS audzēju morfoloģiskais spektrs operāciju un stereotaktisku biopsiju materiālā. Jakovļevs, A., Vanags, A., Gardovskis, J., Štrumfa, I. 2013. gada Zinātniskās konferences tēzes (Rīga, 2013. g. 21.–22. martā) / Rīgas Stradiņa universitāte. - Rīga, 2013. - 267. lpp.